Evaluation of Modern Sedimentation Processes in a Proglacial Lake: Linnévatnet, Spitzbergen, Svalbard

Patrice F. Cobin
pfcobin@mtholyoke.edu
May 2008

Advisor:
Al Werner, awerner@mtholyoke.edu

Committee Members:
Darby Dyar, mdyar@mtholyoke.edu
Jeremy King, jking@mtholyoke.edu

Abstract:

Cores from proglacial lake, Lake Linné, on Svalbard contain varves that hold important information about past climate change. By establishing a relationship between modern sedimentation and measured environmental conditions, we hope to calibrate the late Holocene sediment record found in Lake Linné. Since 2003 sediment trap moorings at five locations in the lake have provided proximal to distal records of overall lake sedimentation. Each mooring also had multiple traps positioned at various water depths, providing insights into the sediment distribution processes in the basin. Trap data show a clear proximal to distal decrease in sediment accumulation and grain size. The data also show an increase in sediment accumulation and grain size as water depth increases. In the most proximal traps, the finest sediment is found at the trap's bottom in a very thin layer. It is followed by an abrupt increase in particle size, which grades to the coarsest sediment found in each trap. During May of 2007, prior to the spring melt, sediment traps were deployed, and an automated camera was set-up to take pictures of the inflow into the lake. The spring traps do not record any of the fine sediment found in the bottom of the yearly traps, suggesting that the majority of sediment in the yearlong traps was deposited during/after the spring melt. In addition to the spring traps and camera, snow sensors and meteorological data associate the abrupt increase in particle size with the loss of the snow pack during the spring melt. After the loss of the snow pack, other pulses of coarse sediment are linked to rainfall events in the valley. In contrast, the sediment collected at the top of the traps in July and August, the height of the ablation season, has a finer texture (fine silt and clay). These findings are consistent with data from previous years, suggesting that for systems like Lake Linné, silt laminations are related to high stream discharge events, resulting from the loss of snow pack and large rain events. The annual clay layer thickness is related to the amount of annual glacier ablation, indicating that the thickness of the clay laminations in the lake cores may be the best proxy for reconstructing late Holocene glacier mass balance. The thickness and the texture of the corresponding silt laminations are related to the environmental conditions, sediment that is remobilized in the fluvial system during high discharge events.

Acknowledgements:

Al Werner made this project possible when he provided me with the opportunity to work this past summer with him and his colleagues, Steve Roof and Mike Retelle, in Svalbard. Al, your continued guidance, support, and humor throughout the past year has made completing my contribution to the Svalbard REU project possible. Thank you for continuing to open up Geology for me in new and thought provoking ways. I would also like to thank Steve, Mike, Megan Arnold and Matthew Moore whose hard work helped make the summer 2007 field season both possible and enjoyable.

I want to extend a special thanks to Darby Dyar and Jeremy King, my advisors since sophomore year. Darby, thank you for inspiring me to become a Geologist, and for your unwavering support over the years (even if I was a bit clumsy in the beginning). Jeremy, thank you for reminding me why I love history so much, and for your tenacity in helping me with my writing - a gift that will follow me throughout my life.

Mom, Dad, thank you for everything. Especially for your steadfast support in all my endeavors, regardless of your worries for my personal safety during my travels! Where I am today has been made possible by you.

Thank you Sarah Beth Cadieux and Erica Emerson, for your friendship and late night pep talks over the past couple of months. However we would have survived this experience without each other…I am glad I do not know. Thank you also to the rest of my friends and family at home, but also to the friends and family I have found in the MHC Geology Department.

The funding for this project was provided by the National Science Foundation Research Experience for Undergraduates, the MHC McCulloch Center for Global Initiatives, and the MHC Geology Department.

Thank you.

Table of Contents:

Table of Figures:

Table of Tables:

Chapter 1:

Background

I. Introduction

The varved lake sediment from Linnévatnet (Lake Linné), Spitzbergen, Svalbard, Norway contains information pertinent to today's changing climate. Numerous studies have been conducted in Linnévatnet to better understand the lake's dynamics, and how it records past climate changes. Many of these studies have been completed as a result of National Science Foundation Research Experience for Undergraduates on Svalbard (REU). The most relevant studies to this project have been conducted in successive years, monitoring yearly sedimentation: 2003-2004, 2004-2005, and 2005-2006.[1]

This study continues to monitor the sedimentation in Linnévatnet, for the 2006-2007 year. AS a result of more instruments in the valley and in the lake, this study is able to more strongly correlate measured environmental conditions to actual sedimentation patterns noted as a result in lake water turbidity and grain size changes. In addition to furthering the understanding of which processes deposit what kind of sediment, different traps were deployed in May 2007 to evaluate if the traps currently used accurately represent deposition. This study also investigates various lab techniques used to evaluate and interpret the sediment, which affect the conclusions drawn about the modern processes in Linnévatnet.

---

[1] Roop, H. *Sedimentation in a proglacial lake: interpreting inter and inta-annual sedimentation in Linnévatnet, Spitsbergen, Norway*. B.A. Honor Thesis, Mount Holyoke College, 2007.
MvKay, N. *Characterization of Climatic influences on modern sedimentation in an Arctic lake, Svalbard, Norway.* Geological Society of America. Abstracts with Programs. 37 (1):29. 2005.
Motley, J. *Sedimentation in Linnévatnet, Svalbard during 2004-2005: a modern process study using sediment traps*. B.S. Thesis, Bates College, 2006.

II. Project Site

i. Svalbard

Located north of Norway above the 74° latitude, glaciers cover two-thirds of the 62,160km^2 Svalbard archipelago, of which the island of Spitsbergen, home to Linnévatnet, is the largest (Figure 1.1). Because they have dominated the landscape for hundreds of millions of years, glaciers have created jagged mountain peaks and fjord systems, except along the coasts, which are characterized by marine deposits on lowlands/strandflats, and raised beaches.[2] The majority of Spitsbergen inland glaciers are cold-based, moving only 1-2 m per year. Closer to the more humid coasts, the glaciers tend to move 10-30 m per year.[3] Like Linnébreen (Linné Glacier), many of Svalbard's glaciers are controlled by snow drift, and are consequently facing downwind, NNW and NW.[4]

The mean annual temperature ranges from -6 to -15 °C, depending on elevation, with the majority of precipitation falling as snow, typically at higher elevations. April and May tend to be the driest period in the year, with February through March and August through September being more humid. Of course, there are years with very different amounts of precipitation and temperatures.[5]

Falling within the zone of continuous permafrost, much of the land area not covered in lakes or glaciers is covered by permafrost and other periglacial

---

[2] Ingólffsson, Ólafur. 2008. Outline of the geography and geology of Svalbard. http://www.hi.is/~oi/svalbard_geology.htm. (accessed February 29, 2008). 1.
[3] Ingólffsson, 2.
[4] Ingólffsson, 2.
[5] Ingólffsson, 1.

features, such as pingos and rock glaciers.[6] Permafrost thickness ranges from 10 m to 450 m plus at higher elevations.[7]

Due to its location, Svalbard has experienced an accelerated warming, like the rest of the Arctic as a result of Global Warming. Arctic temperatures have increased almost 2 °C for every 1 °C of increase in the global average.[8] Like most glaciers, Linnébreen has been retreating in recent decades.

---

[6] Ingólffsson, 2.
[7] Ingólffsson, 2.
[8] Intergovernmental Panel on Climate Change (IPCC) 2007. Climate Change 2007: Synthesis Report. Valencia, Spain, 12-17 November 2007. http://www.ipcc.ch/pdf/assessment-report/ar4/syr/ar4_syr.pdf (accessed May 2, 2008).

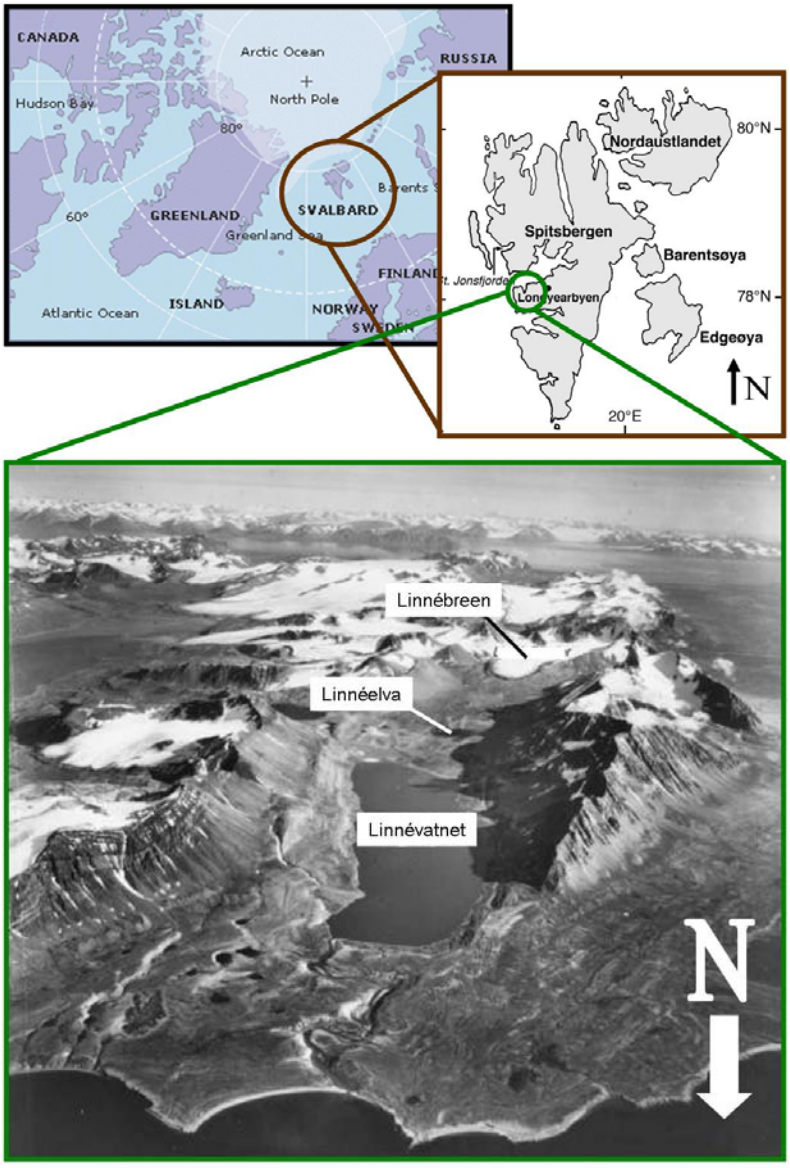

Figure 1.1: Map showing location of Svalbard in the Arctic, as well as Linnédalen, the field work site. (Oblique aerial photograph Courtesy of Norsk Polarstitutt).

ii. Linnédalen (Linné Valley)

Linnédalen is located at the mouth of Isfjord, one of the prominent East-West fjords on the island of Spitzbergen along the west coast of Svalbard (Figure 1.1). Linnévatnet (Lake Linné) sits in Linnédalen and trends N-S, just east of the west coast, at coordinates 78°03'N and 13°50'E. Linnévatnet is a proglacial lake fed by melt water from Linnébreen (Linné Glacier) via Linnéelva (Linné River), and also by smaller side valley glaciers and the 27 km^2 drainage basin (Figure 1.1).[9] Linnévatnet sits about 6km south of Linnébreen, and covers about 8km. Linnévatnet stands 12m above sea level, and is 4.7 km long and 1.3 km wide (Figure 1.1).

Linnébreen was created by repeated glaciations throughout the Quaternary. Following the last deglactiation after the last Glacial Maximum 12,300 yr BP, Linnédalen was connected to Isfjord as a small island.[10] Linnévatnet remained connected to Isfjord until isostatic rebound disconnected the lake from the ocean.[11] Linnévatnet is estimated to have been separated from the ocean around 9500 yr BP, based on the approximate age of a marine terrace between the north end of the lake and Isfjord.[12]

Linnévatnet consists of three basins: the East basin, approximately 16 m deep, the West basin, approximately 11 m deep, and the Main basin, approximately 35 m deep (Figure 1.2). Between the East and West basin is a

[9] Snyder, 2000.
[10] Snyder, 2000.
[11] Snyder, 2000..
[12] Snyder, 2000.

bathymetric ridge (<4m) isolating lake circulation into that potion of the lake (Figure 1.2).[13] Through acoustic profiling of Linnévatnet, it is known that the majority of sediment deposition occurs in the south end of the lake in the east basin.[14] This accumulation indicates a counterclockwise sense of circulation of the water in the lake, flowing from the East Basin to the Main, then into the West Basin.[15]

[13] Snyder, 2000.
[14] Svendsen et al., 1989.
[15] Snyder, 2000.

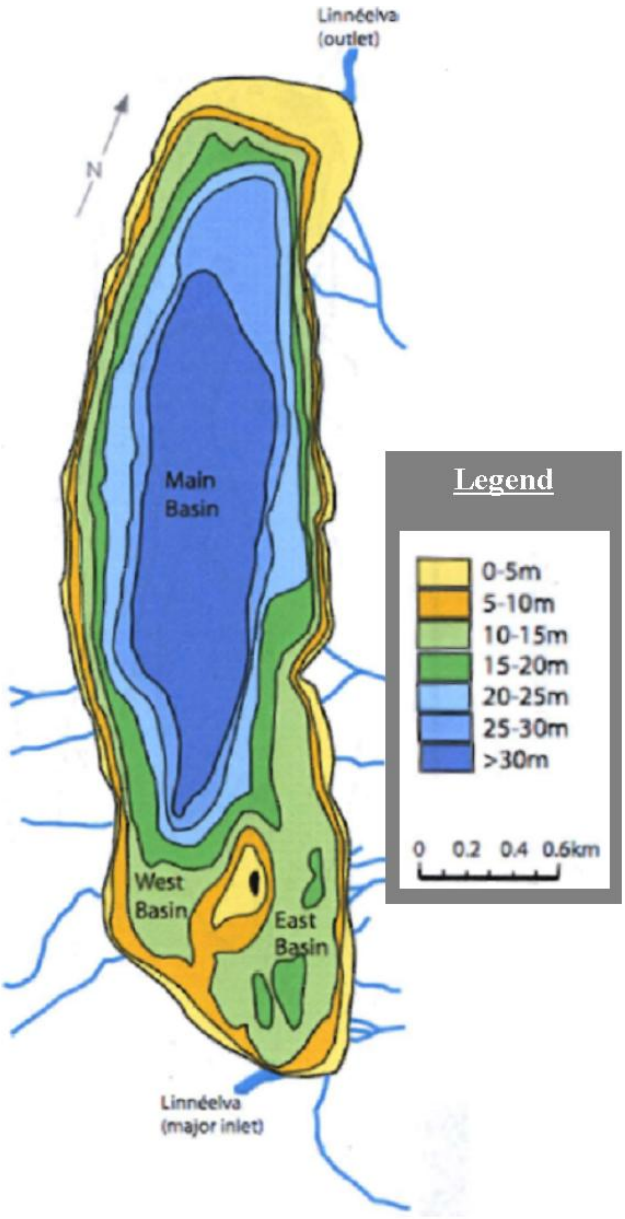

Figure 1.2: Bathymetric Map of Linnévatnet
Map showing lake depths, and the three basins in Linnévatnet: East, West and Main. Note the bathymetric high between East and West. (Figure from Perrault, 2004).

iii. Local Geology

Linnébreen sits upon and erodes lower Carboniferous sandstone. This erosion contributes detrital coal to the lake, such that sediment samples from the inflow stream have moderate carbonate contents (3-6%) and relatively high organic matter content.[16] The western shore of the lake is constrained by the Precambrian-Ordovician Hecla Hoek Complex, a low-grade phyllite rock.[17] The eastern shore of the lake is dominated by Carboniferous-Permian limestone.[18] Gypsum is also detected in sediment samples from the eastern shore of the lake.[19]

iv. Linnévatnet Cores

Lake cores from Linnévatnet show varves (Figure 1.3). These varves, alternating silt and clay layers or couplets of silt and clay representing one year of deposition, are used to count how many years a core represents. A 2006 study associated 12 years with approximately 5 cm of varves, showing yearly couplets counting back to the early 1960s (Figure 1.3).[20] This lake core was taken from a cite near Mooring C.

Besides using the varves to count years, and correlating sediment load, meteorological and lake conditions to varve thickness and grain size to evaluate the sediment processes in the valley, the varves could potentially be used to reconstruct glacier activity. By using sediment traps, we hope to identify the glacier ablation signal created in the deposited sediment by a retreating

---

[16] Snyder, 2000.
[17] Snyder, 2000.
[18] Svendsen et. Al, 1989.
[19] Snyder, 2000.

Linnébreen. Understanding the glacier ablation signal may translate into being able to identify changing glacier mass balance in the lake cores, especially useful for the period known as the Little Ice Age (a time of glacier aggradations occurring globally from approximately the 14th to the 19th century[21]) when Svalbard was ice-locked, unreachable by humans, resulting in no historical observations as to glacier activity. By determining the signals of different depositional conditions today, thereby isolating the glacier ablation signal in the varves, we may be able to identify periods of glacier aggradation in the cores. This study had the potential to allow for a better understanding of the climate changes that are now occurring.

---

[20] Pratt, 2006.
[21] Nesje, Atle and Dahl, Svein Olaf. 2000. Glaciers and Environmental Change. London: Arnold. pg 144.

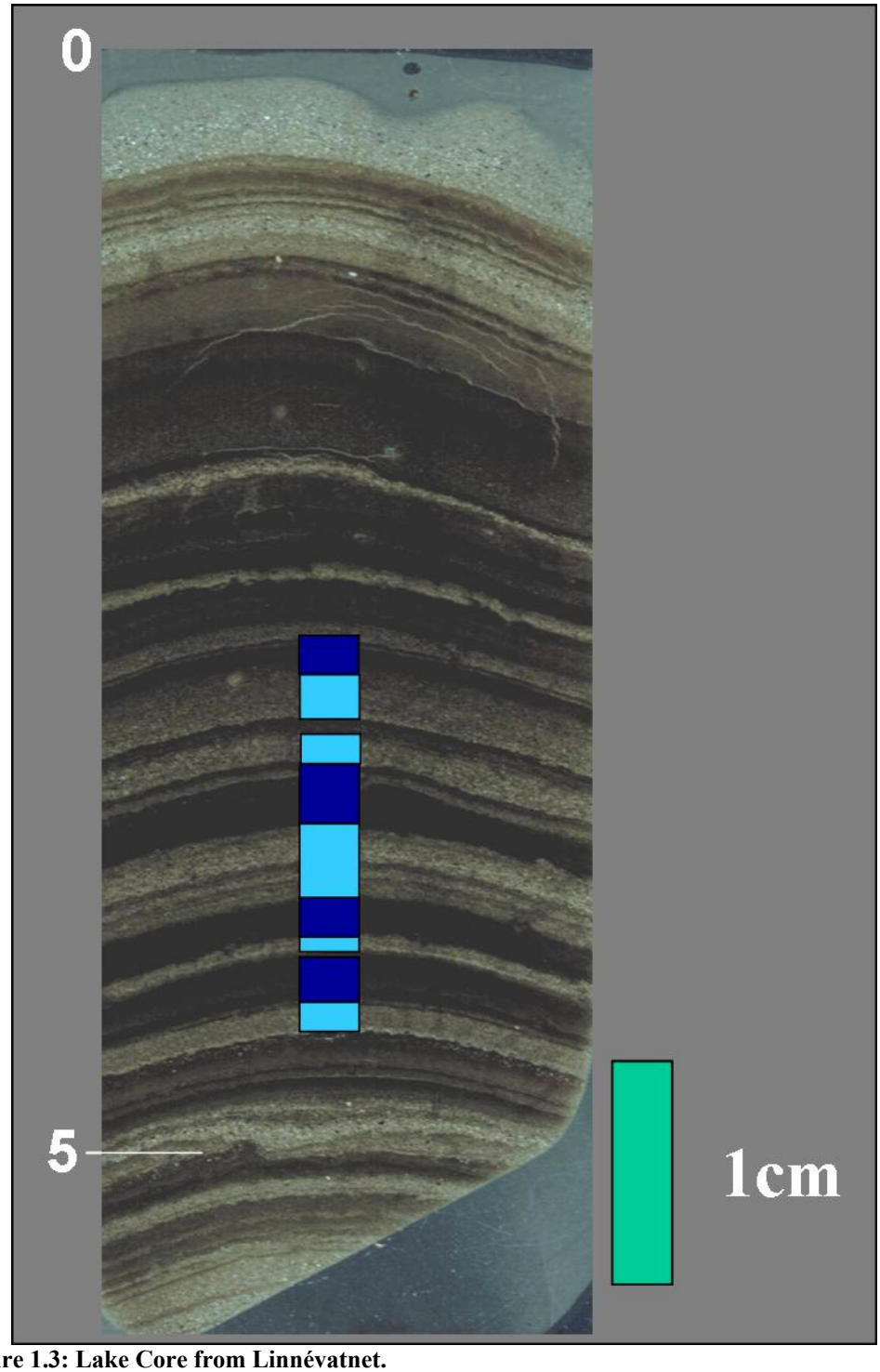

Figure 1.3: Lake Core from Linnévatnet.
A Linnévatnet core showing varves, 5 cm covering approximately 12 years.

III. Sediment Trap Efficiency

The range of possible sediment trap designs used to monitor sediment deposition in a modern environment is extremely varied. While the traps used yearly in the attempt to calibrate Lake Linné have remained constant, ensuring that the yearly results can be compared effectively, their overall efficiency in being representative of what would be accumulated in the absence of the traps is not known. A trap of different design could well show different results in this lake. The design currently in use, as described in Chapter 2, takes advantage of a funnel shape and baffle in an attempt to most accurately represent sediment deposition.[22] Because the efficiency of currently used trap design is unknown, modified traps were deployed in May 2007.[23] By changing funnel shape and removing the baffle, it is hoped that efficiency of the currently used design, the traditional traps, can be better quantified. By quantifying the efficiency of the traditional traps within Linnévatnet, the design can potentially be improved, if necessary.

IV. Sedimentation Processes in Glacier Fed Lakes

One of the biggest uncertainties in evaluating modern sedimentation processes within a proglacial system lies with what happens once the inflow stream, carrying sediment, reaches the lake. We know the different ways sediment can be brought to the lake. But once these streams enter a comparatively motionless body of water and deposits its sediment as it slows,

[22] Roop, 2007. See Roop's discussion on sediment trap designs.

does the inflow water mix uniformly with the lake water? Or does the inflow water seek the depth in the lake that shares its temperature and density, creating over-, inter- or underflows?

Once water enters the lake, it slows exponentially, mixing with the lake water and producing turbidity flows that can expand both 2-dimensionally and 3-dimensionally.[24] At what depth this expanding, decelerating plume enters the lake and deposits its sediment most importantly relies on the density[25] of the incoming water and the density stratification of the lake.[26] If the incoming water is less dense than the lake water overflows occur; more dense then underflows occur.[27] If the incoming water falls between the denser colder water of the lake bottom, and the less dense surface water, the inflow water will follow the thermocline and create an interflow.[28] If the lake is unstratified enough, homopycnal flows will result, meaning that the incoming water mixes with the whole water column of the lake, homogenizing with the lake water.

V. Previous Works

Most relevant to this study are the works done in the past couple of years, which observe previous year's sedimentation in Linnévatnet, 2003-2004, 2004-2005 and 2005-2006.[29] All these studies identified the primary deposition period

---

[23] Design of modified traps described in Chapter 2: Methods.
[24] Benn, Douglas I. And Evans, David J.A. 1998. Glaciers & Glaciation. London: Arnold. pgs. 284-285.
[25] Water is densest at 4°C.
[26] Benn, 1998. pg. 284.
[27] Benn, 1998. pg. 284.
[28] Benn, 1998. pg. 284.
[29] McKay, 2005, Motely, 2006 and Roop, 2007.

for the lake as occurring after the spring melt. Due to the available information from these studies, I was only able to compare my work to results from the 2005-2006 sediment year.[30]

[30] Roop, 2007.

Chapter 2:

Methods

I. Sediment Traps

To continue to create a calibration for Linné lake cores, year-long sediment traps were deployed from 14 August, 2006 to 23 July, 2007. The year-long traps used were the same design (and in most cases the exact same traps) used in previous lake sedimentation studies of Linnévatnet. In addition to the yearlong traps, two more sets of traps were deployed on May 16th and 17th of 2007 (spring traps), and retrieved at the same time as the year-long traps. The first set utilized the same design as the traditional year-long traps. The results of the traditional spring traps, when compared to the year-long traps, provide some time control on sedimentation in the yearlong traps, if trap stratigraphies can be confidently correlated. The design of the second set of spring traps was modified, so that the efficiency of the traditional year-long traps could be evaluated.

All the traps were retrieved by using GPS coordinates to get to the general area of the target moorings. We then motored across the area in a systematic manner, looking over the sides of the boat, and used a Lowrance fish finder until we located the mooring. We snagged the mooring with a chain, and pulled the mooring up using a pulley system (Figure 2.1). Each trap was removed as the mooring was pulled up, held vertically, and transported to shore, where the receiving tube was removed, photographed, measured, described and stored vertically.

Figure 2.1: Pulley System on Boat
As the mooring was pulled up via the pulley system, each trap was removed from the mooring line

i. Year-Long Traps

a. Year-Long Moorings

To monitor the spatial distribution of sedimentation in Linnévatnet, five mooring sites were established prior to this study in the East and West sub-basins and in proximal to distal locations relative to the primary inflow of the lake. The most proximal mooring, Mooring C, is located 0.4 km north of the inflow in the east basin, where the water depth is 15 m (Figure 2.2). Mooring D, more distal, is 0.6 km North of C (1km from the inflow) in the east basin, is located where the water is also 15 m deep (Figure 2.2). Mooring E is situated on the bathymetric high between the East and West basins, about 0.4 km off the south shore, and is 5m deep (Figure 2.2). Mooring F, 10 m deep, sits squarely in the depocenter of the West basin, 0.6 km east of the west shore and 0.4 km from the south shore

(Figure 2.2). Mooring G, 36 m deep, is located the most distally from the main inflow, and lies in the main basin (Figure 2.2).

In addition to monitoring the spatial distribution of sedimentation, each mooring has multiple traps at different depths to record the vertical distribution of sediment within the lake. The number of traps on a mooring depends both on the water depth of each mooring site and the proximity of the location to the main inflow stream.

Every mooring is anchored with a heavy rock to which a nylon rope of appropriate length is securely tied (Figure 2.3). A 10" buoy-ball is attached to the top of the rope to keep the rope taut throughout the year. The rope length at a given location is adjusted to ensure that the buoy stays 1 to 2 m below the lake surface and lake ice.

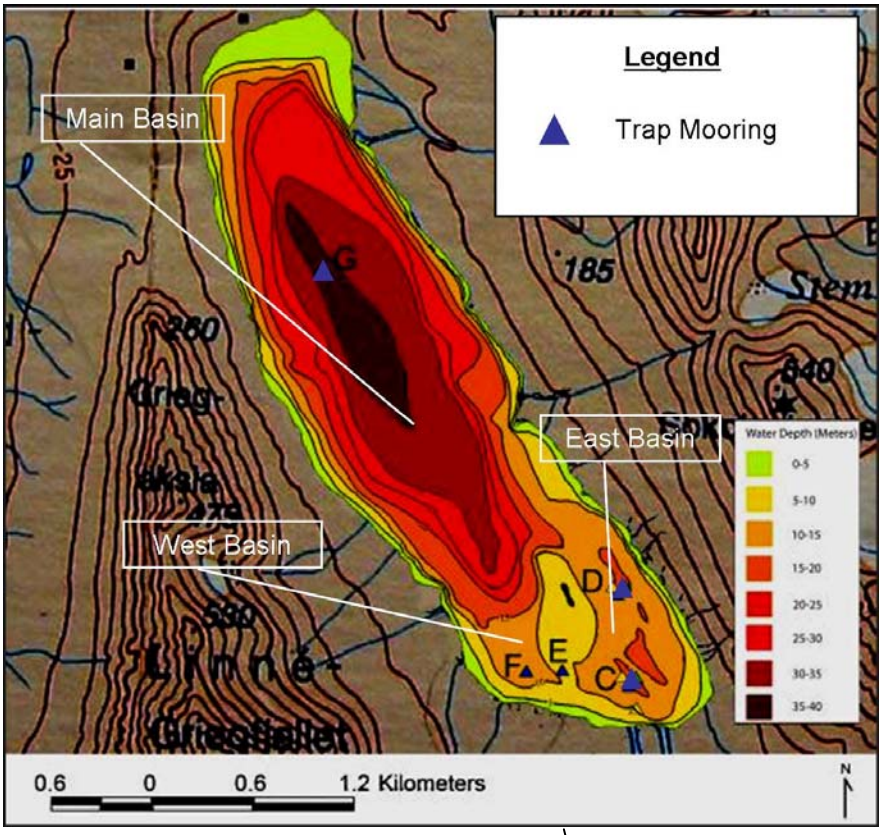

Figure 2.2: Bathymetric Map
Bathymetric map of Linnévatnet, with the lake basins and moorings marked.

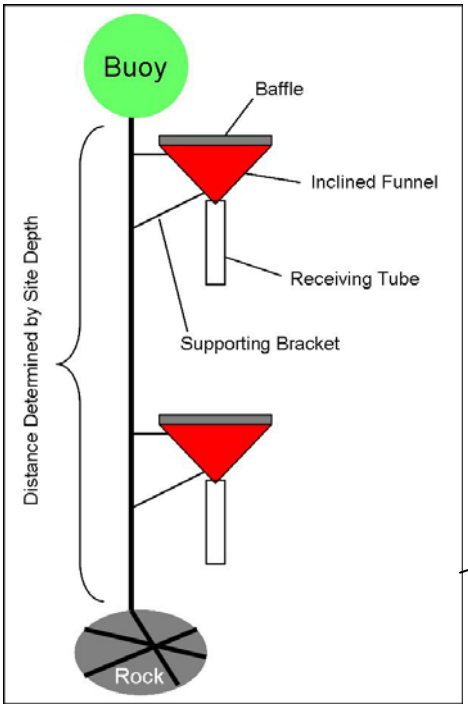

Figure 2.3: Design of Moorings and Year-long Traps
Schematic diagram, not to scale, of the mooring design. Here the mooring is shown with the year-long traps.

b. Year-Long Trap Design

All the year-long traps have a receiving tube, funnel, and baffle. The diameters of the polycarbonate receiving tubes are 1.58 mm and the length of the receiving tube is based on the trap location and the amount of sediment collected at each locality in previous years. The receiving tube is taped to a funnel and a 1 cm^2 baffle is zip-tied to the top of the funnel (Figure 2.3) to minimize the re-entrainment of sediment once it has entered the funnel. The area of the funnel opening is 120.7cm^2. Each complete trap is attached to a bracket (to stabilize and orient the traps) and is then secured to the mooring rope with zip-ties. If properly secured, the traps will be recovered in the same upright manner in which they were deployed.

c. Year-Long Trap Distribution

Mooring C has four traps, C1, C2, C3 and C4 (Table 2.1).[31] Previous work[32] has shown that Mooring C is more sensitive to sedimentation events. Thus emphasis is placed on the data resulting from this suite of traps. Mooring D also has four traps, D1, D2, D3 and D4 (Table 2.1). Mooring E (bathymetric-high) had two traps, but the upper one, E1, was not viable due to a small fish getting trapped in the tube, leaving only the bottom trap, E2 (Table 2.1). F1, F2 and F3 were from Mooring F (Table 2.1). Mooring G was not only the farthest from the

[31] All the traps, on every mooring, are listed here by increasing depth.
[32] Roop, 2007.
McKay, 2005.
Motely, 2006.

lake's inflow, but was also in the deepest part of the lake, and therefore had the most traps, G1, G2, G3, G4 and G5 (Table 2.1).

Table 2.1: Yearlong Trap Distribution on each Mooring

Mooring C		Mooring D	
Trap	Distance Below Surface (m)	Trap	Distance Below Surface (m)
C1	3	D1	3
C2	6	D2	6
C3	10	D3	10
C4	14	D4	14
Mooring E		Mooring F	
Trap	Distance Below Surface (m)	Trap	Distance Below Surface (m)
E1	2.5	F1	3
E2	4	F2	6
		F3	9
Mooring G			
Trap	Distance Below Surface (m)		
G1	3		
G2	10		
G3	20		
G4	30		
G5	35		

ii. Spring Traps

a. Spring Moorings

Each year-long mooring had a spring mooring counterpart, except mooring F. All the spring moorings had only basal traps; spring mooring C was the only mooring that had a surface spring trap as well. The spring moorings were deployed within 10 m of the year-long traps, in the same depositional setting as the year-long moorings, though far enough away so that neither mooring interfered with the other.

b. Spring Trap Design

Two different types of traps were deployed in the spring. The first were traditional traps, which were of the same design as the year-long traps, except that the area of the funnel top was 324.3 cm^2. A larger diameter was used to collect more sediment and thereby amplify the sedimentation record. Additionally, two types of modified traps were deployed at the bottom of spring Moorings C and G to test the trapping efficiency of the traditional traps The modified traps used a 2 liter soda bottle by cutting off the bottom of the bottle, leaving an 84.9 cm^2 opening (Figure 2.4). One modified trap had a 1 cm^2 baffle attached, while the other had no baffle, called Cb and Cnb, respectively (Figure 2.4). The receiving tubes for the modified spring traps were 3.06 mm in diameter, larger than their traditional trap counterparts. All the spring traps were attached to the mooring lines in the same manner as the year-long traps.

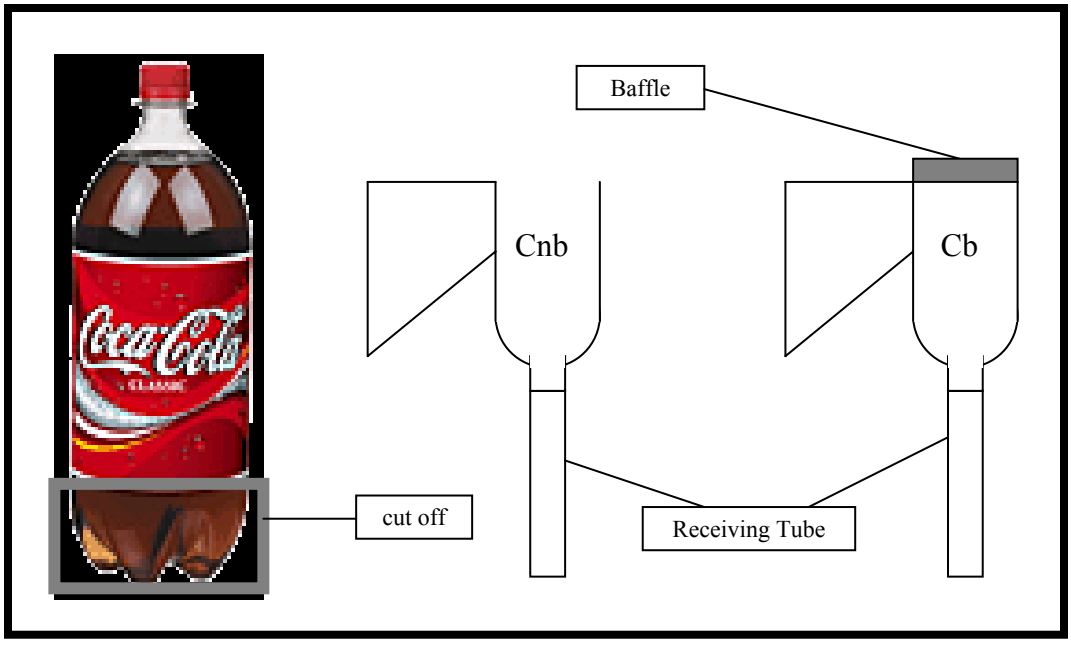

Figure 2.4: Modified Spring Trap Design
A picture of a Coca-Cola bottle showing the portion of the bottle that is removed to create the funnels. On the right is a schematic drawing of what the traps look like once the bottle has been modified.

c. Spring Trap Distribution

Spring mooring C had four traps: two traditional traps, one at the top (Cs), and one at the bottom (Cbt), and two modified traps, one with a baffle (Cb) and one without (Cnb) (Table 2.2). Spring traps Cbt, Cb, and Cnb were at the same depth. To accommodate one another they fanned out around the nylon mooring rope. Spring mooring D had only a traditional spring trap at the top (Ds) and bottom (Dd) of the mooring (Table 2.2). Mooring E had four traps like C, but due to fish in the receiving tube or something else that compromised the sediment, only the traditional surface trap (Es) was viable on E (Table 2.2). Spring mooring

G had only the modified traps, one with a baffle (Gb) and the other without (Gnb), at the bottom (Table 2.2).

Table 2.2: Spring Trap Distribution on each Mooring

Mooring C		**Mooring D**	
Trap	Distance Below Surface (m)	Trap	Distance Below Surface (m)
Cs	2.5	Ds	2.4
Cbt	14	Dd	14
Cb	14		
Cnb	14		
Mooring E		**Mooring G**	
Trap	Distance Below Surface (m)	Trap	Distance Below Surface (m)
Es	2.5	Gb	35
		Gnb	35

iii. Grain Size Analysis

a. Sub-sampling

To access the sediments within the receiving tubes, a special core cutter was developed in the summer of 2006 by Thomas Liimatainen, the machinist at Mount Holyoke College. The tubes were secured horizontally to a metal rail and cut by a router using a handmade circular blade. The router was also on a rail, allowing the cutter to be pulled smoothly across the surface of the receiving tube. This approach was used in order to minimize sediment disturbance and loss. Two cuts were made to minimize the contamination of the sediment by polycarbonate cuttings. The first was taped over and then the tube was flipped 180° to make the second cut. A thin aluminum sheet was then pushed into the second cut, splitting

the sediment in half, and taped over. The tubes remained securely taped until they were opened for sub-sampling in the lab (Figure 2.5).

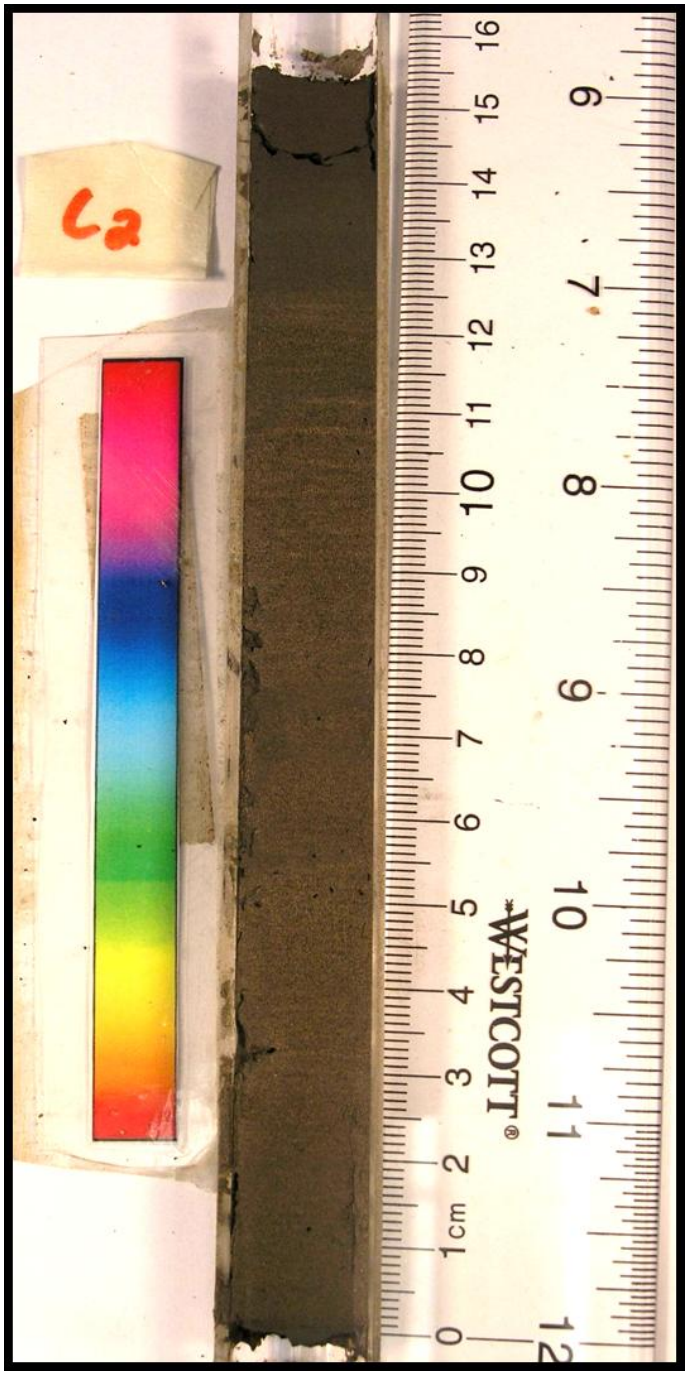

Figure 2.5: A Split Sediment Trap
An example, C2, of a sediment trap once it has been opened. Color differences in the sediment layers can be seen.

b. Visual and X-Ray Stratigraphy

To obtain particle size samples, the best-preserved half of each receiving tube was sub-sampled and placed into individual sampling vials that had been weighed empty. Sub-sampling followed both visual stratigraphy and stratigraphy boundaries observed through the X-ray results (See Results for exact sampling increments per trap). The X-ray data were extremely useful on the sediment traps that had tens of centimeters of sediments, in which the laminations were on the order of millimeters and hard to differentiate visually. Some traps, such as C4, (high sedimentation rate) were sub-sampled in 2 mm increments, independent of observed sample stratigraphy.

Some of the traps had only a few centimeters of sediment that contained stratigraphy boundaries between silt and clay that were particularly steeply inclined. The cause of this inclined bedding is not understood. In these situations, the boundary was preserved by sampling along that steep incline, making the grain size graphs a little harder to read, because the inclination essentially makes two sub-samples for that one layer. In other words, that one layer has a clay layer half, and a silt half. Fortunately the mooring C traps, which are the focus of this study, did not have inclined layers to that degree, simplifying the sampling methods required.

The X-ray analyses were carried out using Kodak film in film canisters designed for fine bones, yielding a higher resolution. One half of every tube was exposed at 3 mA, 30 to 45 kV, and anywhere from 3-5 s. The actual energy and

exposure times depended on the density of the sample, which was directly related to the proximity of the trap to the inflow, and therefore the texture of the sediment found in the trap.

In addition to sub-sampling all the traps according to visual and X-ray stratigraphy, C1.2 (the other half of C1) was sub-sampled at uniform intervals. By sub-sampling one trap two ways, the first honoring stratigraphy, and the other taking the same size samples at regular interval, the two sample methods could be compared to evaluate sampling bias.

The larger diameter of the receiving tubes on the modified spring traps allowed sediment to settle in thinner layers, of similar grain size, than in the narrower diameter traditional traps. As a result, sampling at fine enough intervals to accommodate the thinner layers was not always possible.

It is important to note that all the samples are identified relative to their distance from the bottom of the receiving tube. That distance is the measurement from the top of sediment interval relative to the bottom of the trap. Every sample actually has two measurements, one from the bottom of the sample and one from the top. For example, in trap C1 the first sample is reported to be 2 mm from trap bottom, which really means that the sample of sediment represents what is found from 0 to 2 mm in C1 when the ruler is held with 0 mm at the bottom of trap.

c. Particle Size Analysis

To prepare the sediment for particle size analysis, every sample was placed in a drying oven at 90°F for at least 8 hrs, to ensure the sample was

completely dry before reweighing the vials. Knowing the weight of each vial with and without sediment allowed total sediment mass to be calculated. After the reweighing, each sample was treated with 1 to 3 ml of dispersant, depending on the amount of sediment in each sub-sample. The dispersant was a mixture of 7 g sodium carbonate and 35 g sodium metaphosphate per liter of water.

The Woods Hole Reinhart Coastal Research Center's LS 13 320 Beckman Coulter single wavelength laser diffraction particle size analyzer was used for this study. To prepare the samples for the Coulter Counter, each sample was washed out of its vial with tap water (the machine itself used tap water) and poured into vials designed for the machine. Each sample was sonicated before placing it in the carousel. If the machine did not detect the sediment in the tube the sample was skipped (Figure 2.6).

The Coulter also sonicated each sample two more times to ensure complete dispersion, once before it was poured into the machine, and a second time before average grain size was determined. Once inside the machine, the sample was analyzed through a series of laser diodes and photodetectors. The calculated grain sizes were self-corrected by the machine using a pre-determined calibration. Right before the machine ran, each sample obscurity was determined, with the acceptable amount between 15 and 30%[33]. If obscurity was too high, the machine would add tap water little by little until the numbers were within acceptable limits.

[33] Maya Gomez, Lab Director for the Coulter at Woods Hole Reinhart Coastal Research Center.

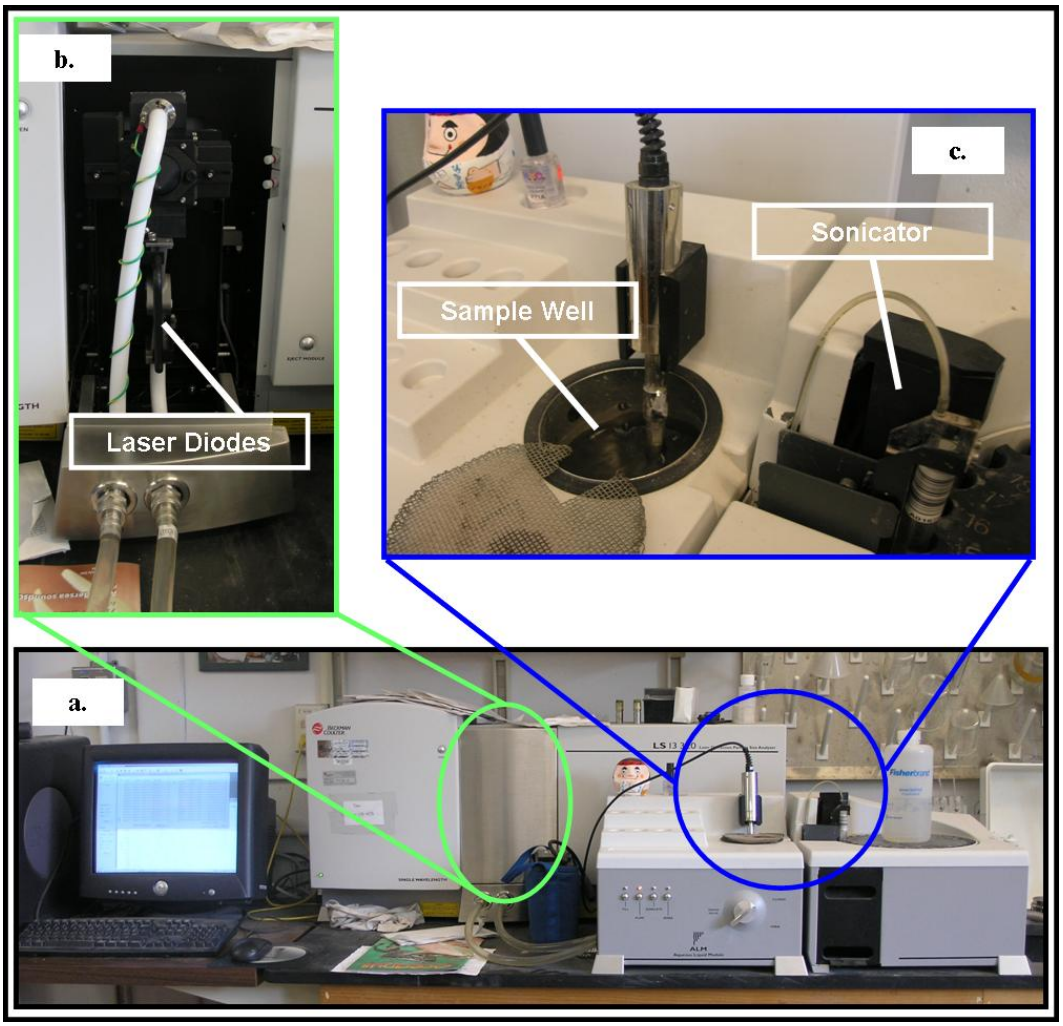

Figure 2.6: Coulter Counter
a.) Coulter Counter and accompanying computer. b.) Location of the laser diodes and photodetectors. c.) Where sample is sonicated then poured into the sample well to be analyzed.

iv. Determining Sediment Flux

To compare the amount of sediment collected from one trap to another, especially the yearlong traps versus their spring counterparts, the data had to be corrected for the magnification of sedimentation associated with each funnel. Previous studies have corrected funnel magnification using the following

method.[34] The "funnel magnification factor" for each trap was calculated using the following equation:

Sediment flux = mass of sediment in each trap in g / area of funnel top in cm^2

or

$$f = m/a.$$

The amount of sediment in each trap was calculated from the weight of the dried sub-samples. Different sized funnels were used in the year-long traps and the two sets of spring traps.

Each trap, no matter where it was located on the mooring, establishes an artificial lake bottom. While all the traps contribute to a better understanding of lake sedimentation processes, the bottom trap on each mooring most closely mimics the actual sediment that would collect on the lake bottom in the absence of the trap. Applying a bulk density conversion to the sediment flux of the bottom traps yields the amount of sediment deposited per year, in units of vertical thickness (mm/yr) [35]:

vertical thickness = (sediment flux/mean bulk density from Linnévatnet) × 10

or

$$t = (f/1.8) \times 10.$$

Mean bulk density (g/cm^3) was derived from the sampling of multiple lake cores at varying depths and locations throughout Linnévatnet.[36] The bulk density conversion is multiplied by ten to convert from centimeters to millimeters.

[34] McKay, 2005.
[35] McKay, 2005.

II. Environmental Data

i. Lake Temperature Data

For the yearlong traps every sediment trap and mooring anchor rock was equipped with an Onset Water Temp Pro logger that recorded temperature every thirty minutes.

ii. Lake Bottom Water Turbidity

An In-Situ Inc. 9000 Pro XP/e Troll was deployed with the spring traps at Mooring C to measure water turbidity, temperature, conductivity, and depth every two minutes, from May 17th to July 23rd, 2007. The troll was set up with its depth comparable to C4 and the spring bottom traps. The turbidity data were calibrated to experimental data obtained by measuring the turbidity of manufactured sediment water mixtures (using sediment from mooring C).

iii. Weather

Using an Onset HOBO weather station, various meteorological parameters were documented in the valley (at thirty minute sample intervals) from 14 August 2006 to 23 July 2007. Most pertinent to this study are air temperature and precipitation measurements, as these directly affect snow and glacier melting and stream discharge in the valley.

iv. River Temperature Data

At two locations in the main inflow stream into Linnévatnet, water temperatures were monitored using Onset Optic Stowaway and Tidbit loggers.

---

[36] McKay, 2005.

The two locations were mid- and lower- stage. Mid-stage was located next to the snow tree (see below) in the river, and the low-stage site was located approximately 75m upstream from the mouth of the river's inflow into Linnévatnet. Measurements were taken every thirty minutes to monitor when the stream completely froze (stopped flowing) and thawed (started flowing) during the spring melt.

v. Snow Tree

At the site of the mid-stream temperature logger, a snow tree was positioned and anchored down for the entire year. The site was chosen because it sat above flood stage and in a small ravine where snow was known to collect. The data collected here are unique to this site and do not represent snow accumulation throughout the valley. However, the results may be considered a time proxy for overall snow accumulation and melt.

The snow tree consisted of four limbs, with a logger attached facing downward on each limb to measure both light intensity (surface albedo) and temperature every thirty minutes. The loggers recorded from August 14, 2006 to July 23, 2007. The limbs were 7, 15, 30 and 45 cm above the ground (Figure 2.7).

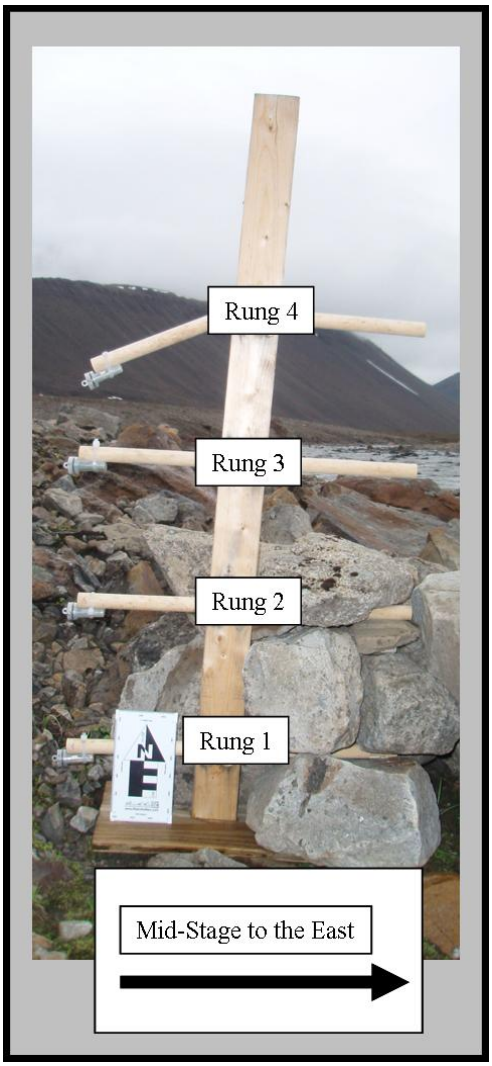

Figure 2.7: Snow Tree Diagram
A picture showing the design of the snow tree. The snow tree was secured with rocks to ensure it stayed vertical. Rung 4 was broken when found.

vi. Automated Camera

A camera was set up at the end of May, along with the spring traps, to take pictures every three hours of the south end of the lake, the inflow stream, and the valley. The camera was located on a ridge along the east bank of the lake, facing roughly SSW (N78 02.220, E13 52.319). Barring a few rain spattered-pictures, the camera recorded the conditions in Linnédalen very clearly.

vii. Lake level

A Solinst levelogger was also deployed late May 2007, prior to the spring melt. It was on the same mooring as the Troll CTD, and measured hydrostatic pressure every thirty minutes. The collected measurements were barometrically corrected by taking the pressure data from the weather station, converting them to their equivalent hydrostatic pressure changes, and subtracting them from the levelogger data to yield actual water-level fluctuations.

Chapter 3:

Results

I. Sediment Traps

i. Year-Long Traps

a. C1 Trap Data

Starting from the bottom of Trap C1, the mean grain size increases to its coarsest point in the first 8 mm, going from 5.17 μm to 16.25 μm (Table 3.1 and Figure 3.1a). The mean grain size then falls slightly to 15.11 μm at the next sampling interval, 12 mm from the bottom, before rising to the second coarsest mean grain size of 15.21 μm at 16 mm from the bottom. Mean grain size falls gradually for the remaining sediment in the trap, reaching 10.60 μm, slightly more than twice the mean grain size found at the bottom of C1.

b. C2 Trap Data

The two instances of coarsening that are weakly present in C1 are more distinctive in C2. The average grain size from the first sampling interval to the second quickly jumps 9 μm to 19.10 μm, where the grain size hovers for the next three sampling intervals, 5 mm to 20 mm from trap bottom (Figure 3.1b). Grain size then increases, creating the first coarsening event in the trap and reaching a maximum average of 23.55 μm. Grain size then falls for the next three sampling intervals before rising slightly to 19.94 μm at 65 mm from trap bottom. Grain size then falls to a low of 18.60 μm at 70 mm, before rising into the second coarsening event, maxing out at 27.70 μm at 105 mm from trap bottom. Like trap C1, grain size then decreases to 11.43 μm at 144 mm after the second coarsening

event. Unlike C1 and C1.2, after the grain sizes fall in C2 they begin to rise again, reaching 14.13 μm at the top of the trap (Figure 3.1b).

c. C3 Trap Data

Trap C3 follows the overall pattern found in C2 except for three noticeable differences: C3 has more sediment overall, grain sizes are coarser, and between the two main coarsening events grain size show more variation (Figure 3.1c). The first coarsening event reaches 26.42 μm at 38 mm, before falling into the peaks and valleys just to rise into the second coarsening event, reaching 34.61 μm at 112 mm. The sediment between the two coarsest peaks extends from 54 mm to 94 mm from trap bottom, and has three peaks, the coarsest being 24.08 μm at 92 mm. After the second coarsening event grain size falls to 11.71 μm at 164 mm, and then increases to 12.34 μm the top of the trap (Figure 3.1c).

d. C4 Trap Data

Traps C4 and C3 mimic one another even more than C2 and C3, but C4 accumulated more sediment, and does not begin to coarsen noticeably for the first 20 mm of sediment in the trap (Figure 3.1d). The two coarsening events in the trap do not have obvious peaks. For the first event, grain sizes reach a maximum of 24.44 μm at 54 mm, and 32.86 μm at 142 mm for the second coarsening event. Between the two coarsest peaks in the trap, from 76 to 117 mm, grain sizes vary as in C3. In this interval, there is a distinctive peak, from 76 to 10mm, that has enough sampling intervals to show an increase and decrease in average grain size

(Figure 3.1d). C4 also has an increase of grain size at the top of the trap after the decreasing limb of the second coarsening event (Figure 3.1d).

e. C1.2 Trap Data

Trap C1.2, the other half of C1 sampled at regular intervals, showed the same overall pattern as C1. Mean grain size quickly rises to the first coarse peak, dipping before rising to the second grain size peak and then gradually decreasing. As in C1, the sediment at the top of C1.2 is coarser than the sediment found at the bottom of the trap. In C1.2, the dip between the two coarsest peaks is accentuated by the finer regular sampling technique. Overall, the differences in mean grain sizes in C1 and C1.2 are considerably small, and are thought to be basically the same (Figure 3.1a).

f. Mean Grain Size versus Median and Mode

All previous studies have used the mean grain size data from the Coulter Counter to evaluate the sedimentation process in Linnévatnet, a practice this study continues. To ensure no misinterpretations are made, a comparison of mean, median, and mode for trap C4 shows that while median and mode have coarser grain sizes the pattern of the line remains the same (Figure 3.2). All the other median and modes for the other traps discussed follow the same pattern as observed with C4, though they are not discussed here (see Appendix for the median and modes of the other traps).

ii. Spring Traps

a. Traditional Surface Trap (Cs) Data

Trap Cs (the spring counterpart to the trap data from C1 and C1.2) does not have the fine-grained interval found in the bottom of the yearly traps. Overall, the grain sizes are coarser at the bottom of the trap, with half of the lowest most peak missing the increase limb, and then they decrease towards the top of the trap (Figure 3.3a). Straying from the overall pattern, there is an anomaly with the second sampling interval. The first interval at 3 mm has a grain size of 13.95 μm, followed by a decrease to 12.07 μm at 4 mm at the second interval, only to increase again at the third interval, also the coarsest of the trap, to 14.04 μm at 7 mm. It is important to note that while the graph shows this as a substantial jump, the grain sizes in the first three intervals are within 2 μm of each other (Figure 3.3a).

b. Traditional Bottom Trap (Cbt) Data

Except for the absence of the fine-grained unit at the bottom of the trap, the traditional spring trap, Cbt, at 14m below the surface, follows the same general pattern found in traps C2, C3 and C4. Cbt has three coarsening events where each successive event in Cbt has a coarser grain size. The three peaks are from 8 to 29 mm, 32 to 64 mm and 72 to 120 mm, with their coarsest grain size being 20.52 μm, 23.96 μm and 31.90 μm, respectively (Figure 3.3b). There is another slight rise at 68 mm, with a grain size of 21.92 μm. Since it is only one point, it could be a result of mechanical error with the Coulter Counter.

c. Modified Traps' (Cb and Cnb) Data (Coke Bottle Traps)

Placed right next to each other, Cnb collected slightly more sediment than Cb. While the mean grain sizes found in each trap mimic one another fairly closely, the decreases and increases in Cnb are larger than Cb (Figure 3.3c). Where Cnb obviously has three peaks like Cbt, the three peaks in Cb are less perceptible. Even so, the coarsest parts of each peak in Cnb and Cb are remarkably similar, and both are similar to the peaks found in Cbt (Figure 3.3c and Table 3.2).

	Cb		Cnb		Cbt	
	Distance from Trap Bottom (mm)	Average Grain Size (μm)	Distance from Trap Bottom (mm)	Average Grain Size (μm)	Distance from Trap Bottom (mm)	Average Grain Size (μm)
1st Peak	8	19.9546	5	19.8869	18	20.52
2nd Peak	20	22.7893	14	22.6193	40	23.96
3rd Peak	33	31.9528	33	30.7672	100	31.90

Table 3.1: Spring Trap Grain Sizes at each Coarsening Peak
The mean grain size found at each peak in each of the deep water spring traps, Cbt, Cnb and Cb. Note the similarity of the particle sizes.

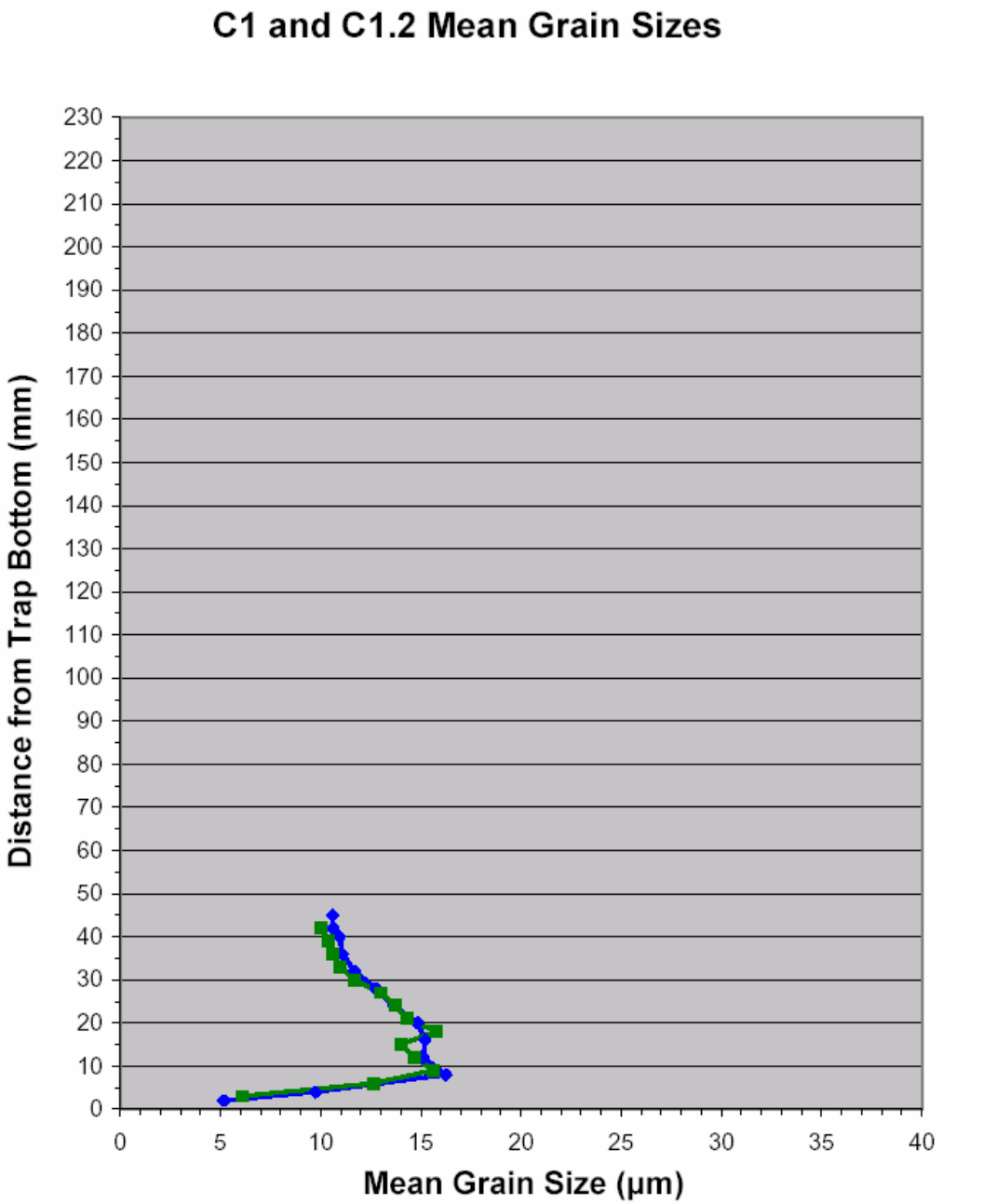

Figure 3.1a: Mean Grain Size for Trap C1 (C1 = blue, C1.2 = green)

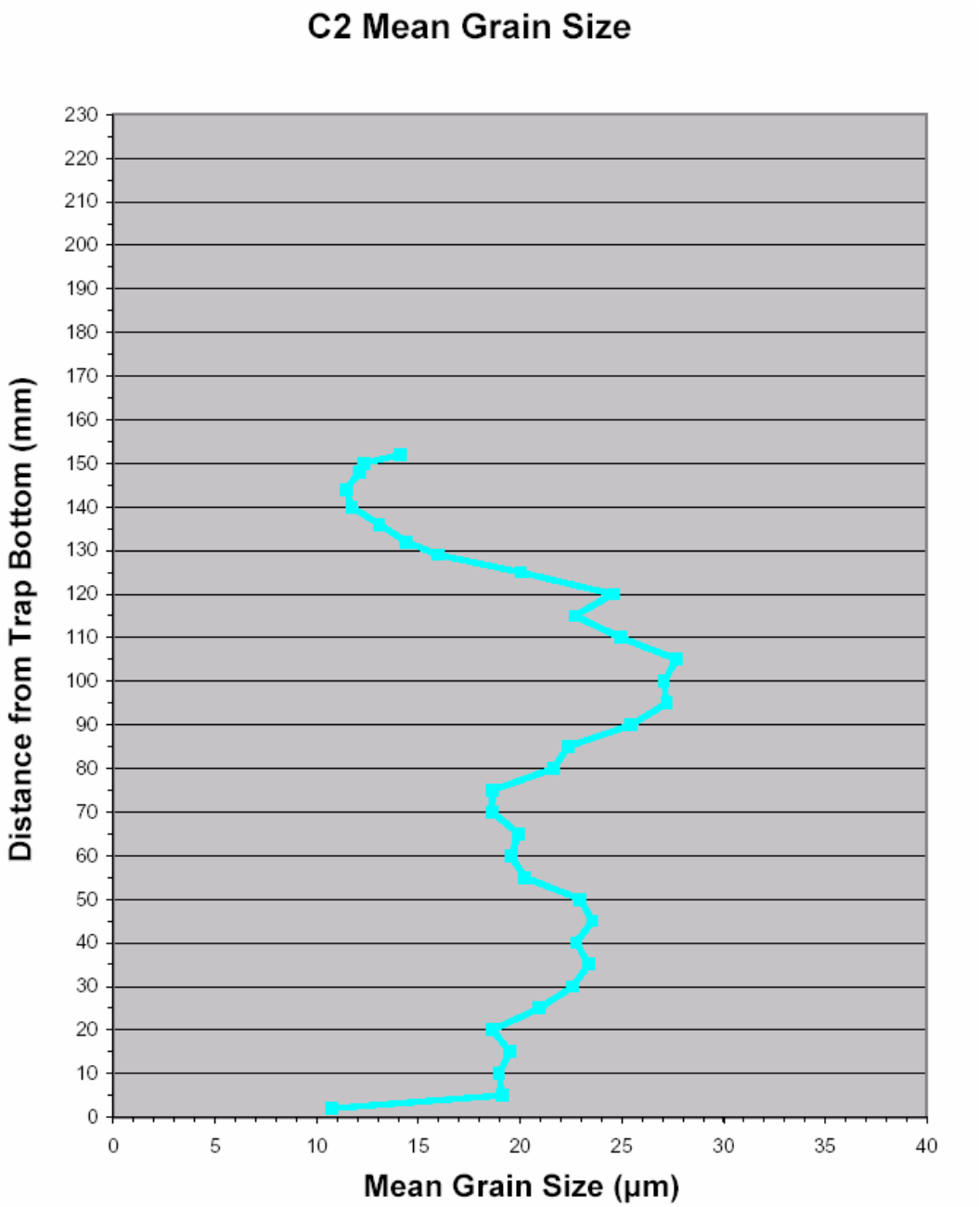

Figure 3.1b: Mean Grain Size for Trap C2

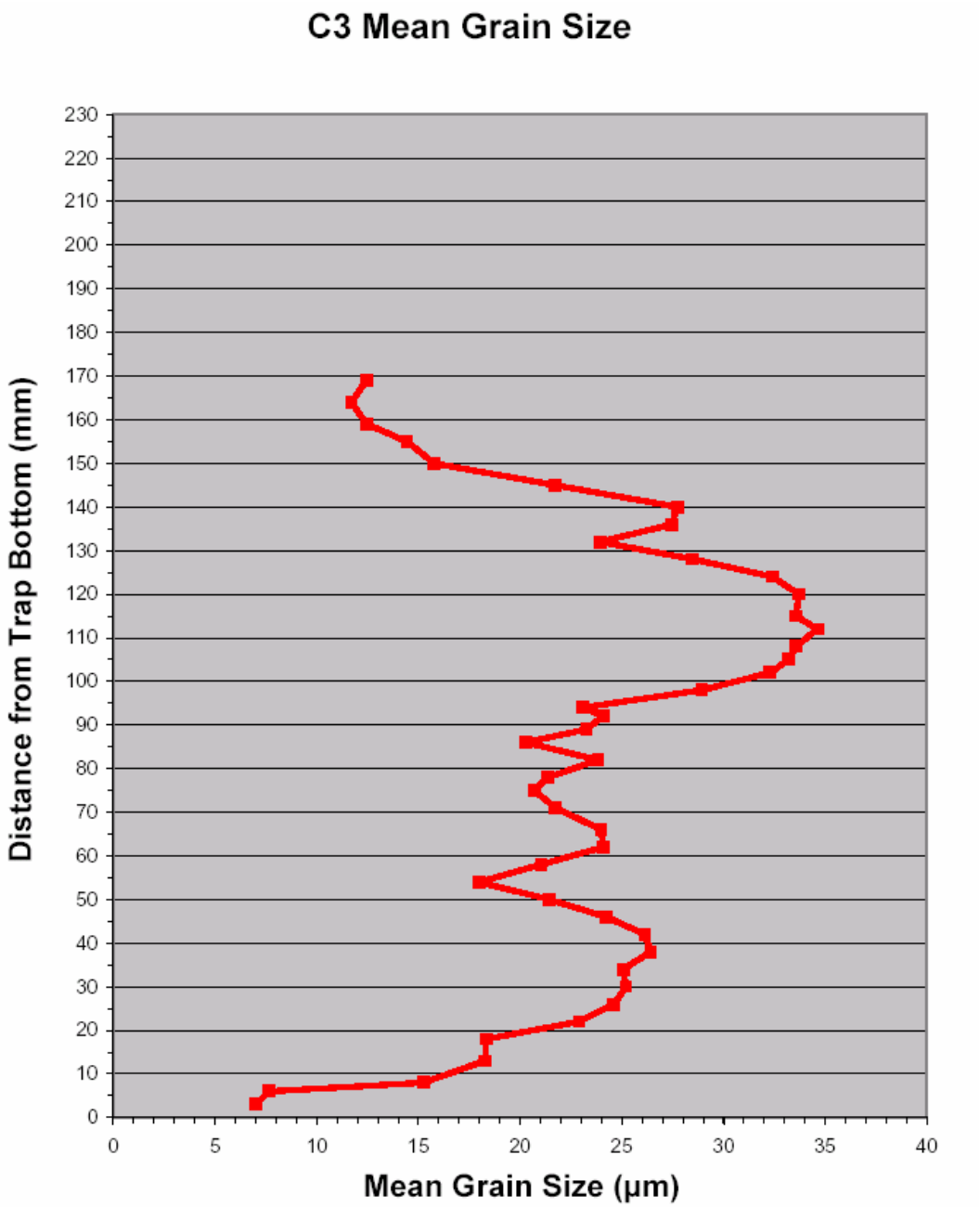

Figure 3.1c: Mean Grain Size for Trap C3

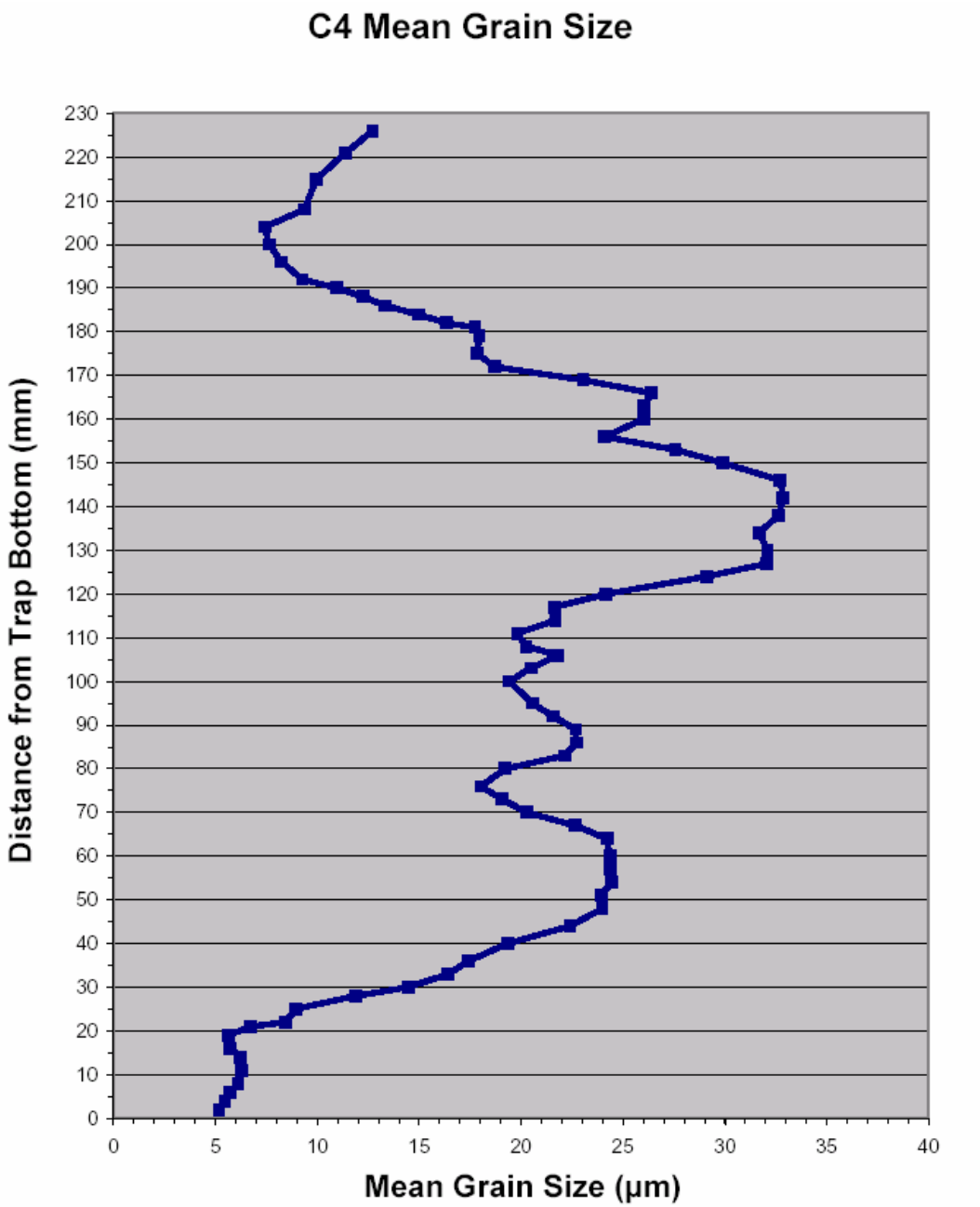

Figure 3.1d: Mean Grain Size for Trap C4

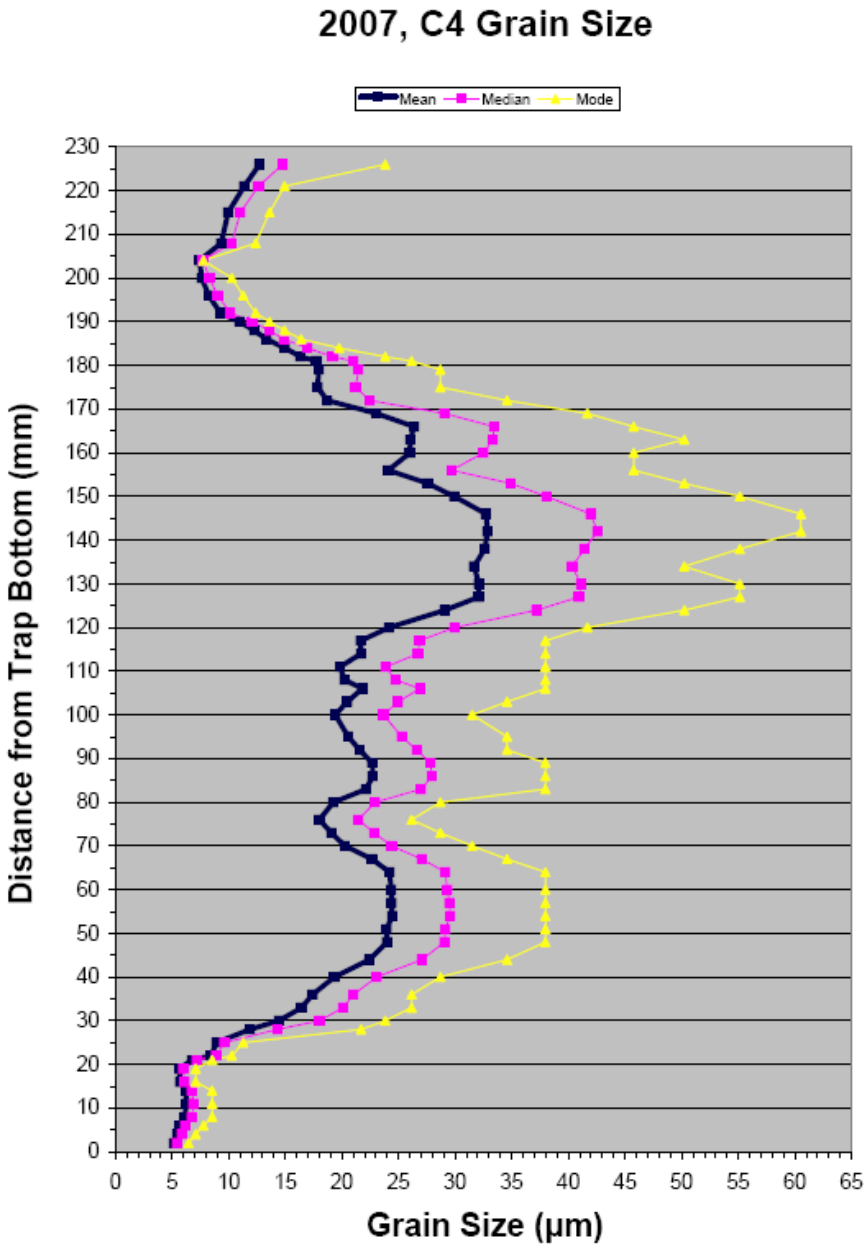

Figure 3.2: Mean vs Median vs Mode for Trap C4 Grain Sizes

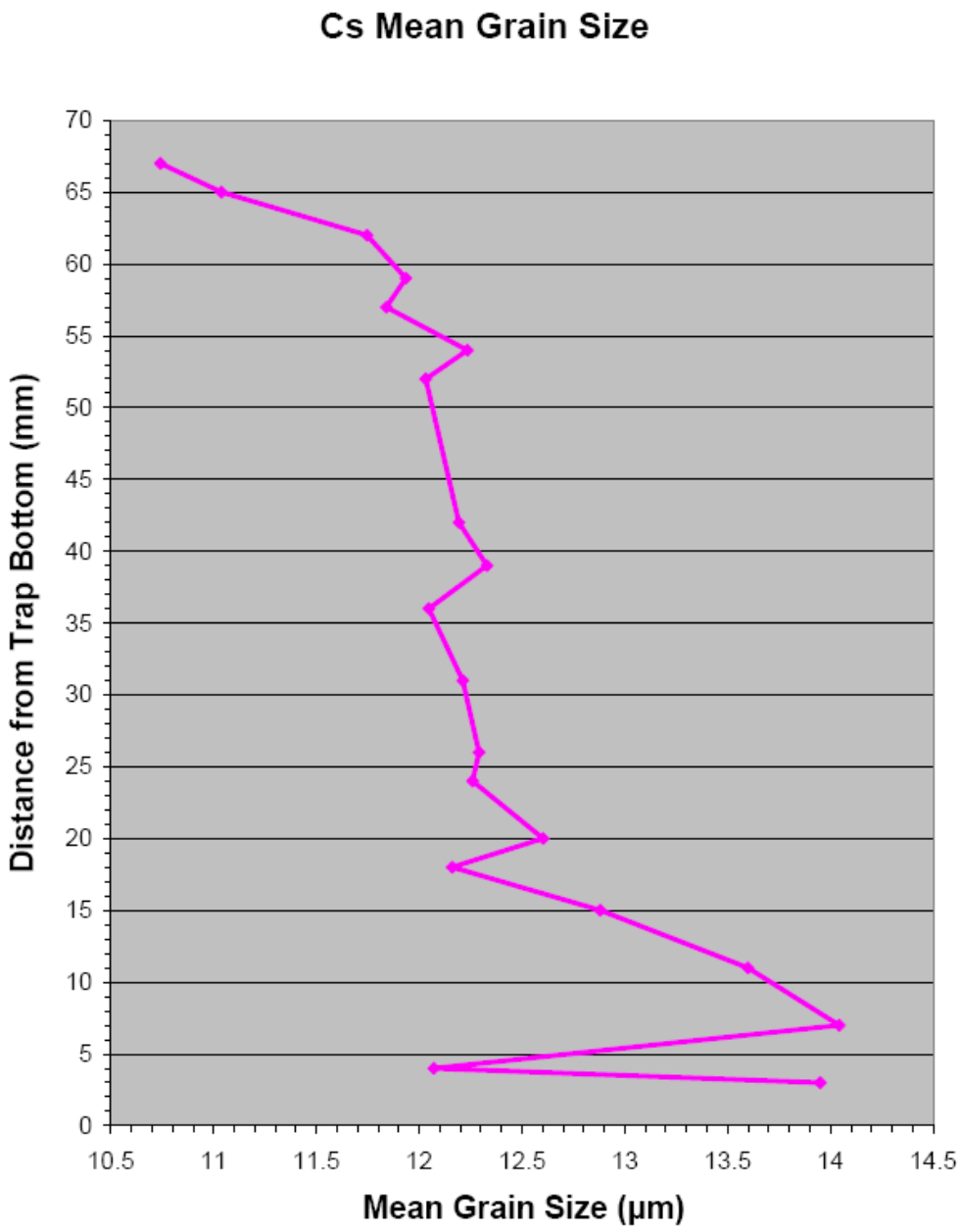

Figure 3.3a: Mean Grain Size for Trap Cs. Please note that the x-axis starts at 10.5 µm and only goes to 14.5 µm.

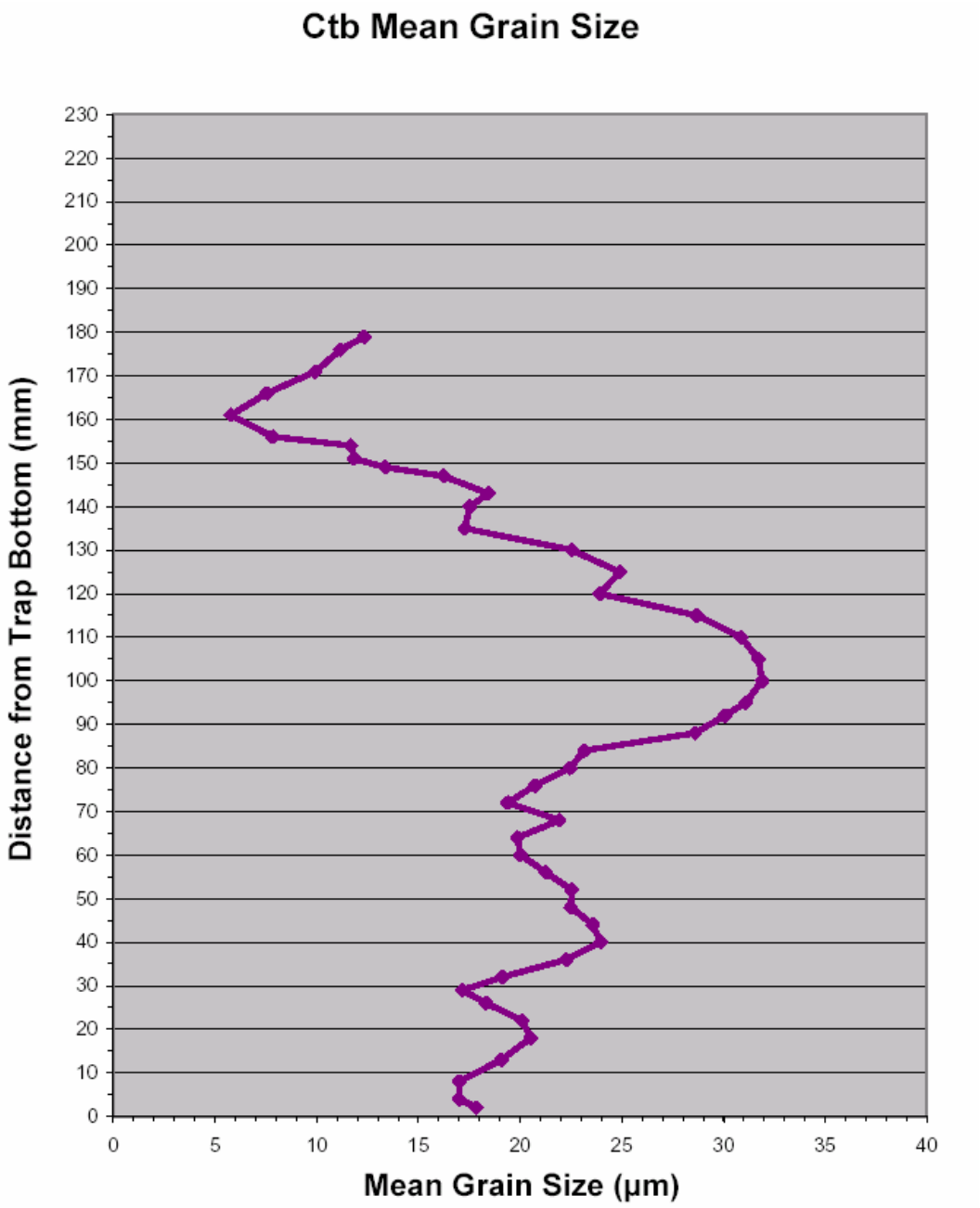

Figure 3.3b: Mean Grain Size for Trap Cbt

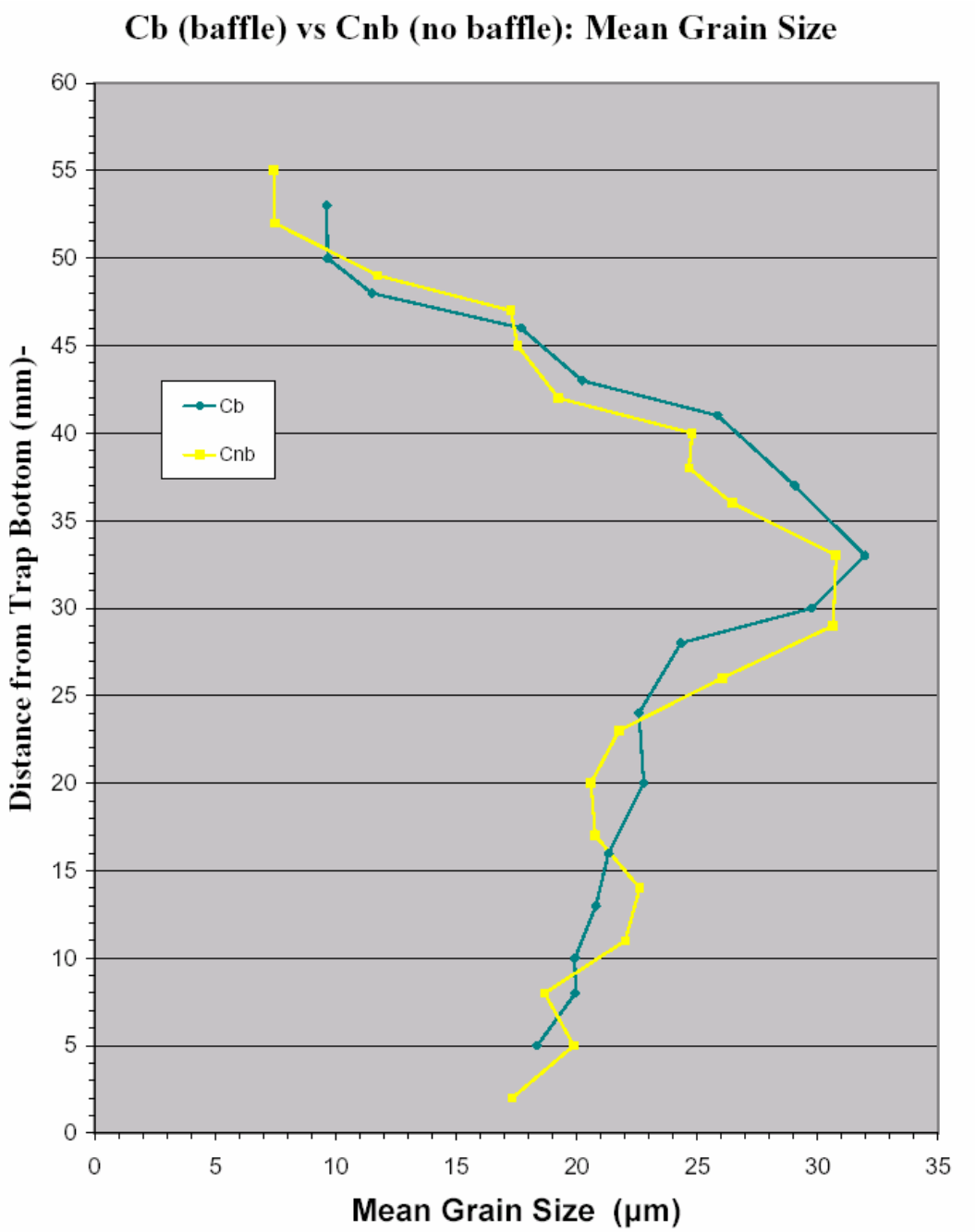

Figure 3.3c: Mean Grain Size for Trap Cn and Cnb (Coke bottle traps).

iii. Sediment Flux

The following table contains sediment flux for traps C1, C2, C3, C4 and Cbt (Table 3.3).

Table 3.2: Sediment Flux

Trap	C1	C2	C3	C4	Cbt
Sediment (g)	12.7918	62.0804	79.3072	111.7316	95.8388
Funnel Area (cm2)	120.7	120.7	120.7	120.7	158.4
Sediment Flux (g/cm2)	0.106	0.514	0.657	0.93	0.605

III. Lake Temperature Data

The water temperature loggers positioned at various water depths at the five mooring locations document the seasonal thermal evolution of the lake and allow inflow events to be recognized. In general, all the loggers followed a general pattern. In late summer, right after deployment, lake temperatures kept mostly within 1 °C of each other, between 5.5 °C and 6.5 °C, throughout the water column. Mid-September found the lake temperatures steadily dropping for the first half of the fall season. Then each trap logger leveled out for duration of the winter months, only to rise again at the end of June (Figure 3.4a).

Late summer lake temperatures from 14 August to 15 September 2006 ranged mostly from 5.5 °C to 6.5 °C. Though on September 13th temperatures at C4 and the rock did drop to almost 4.5 °C, with the rock having colder temperatures than trap C4. C3 had an intermediate temperature, with C2 and C1 being the warmest. C2's temperatures were a less accentuated version of those recorded at C1 (Figure 3.4b).

If the late summer temperatures are considered normally stratified, with C1 being the warmest and C4 the coldest, the temperatures recorded from 14 August to 18 October 2006 show the beginnings of reverse stratification, beginning when C4 temperatures clearly become the warmest around mid September. The loggers at C1 to C4 also begin to follow reverse stratification on 27 September, but they oscillate between reverse and normal stratification of temperatures during the rest of the fall months (Figure 3.4c).

During the winter, from 13 October 2006 to 30 June 2007, the temperatures of the moorings were reversely stratified, except for C3. C1 had the coldest temperatures, which C3 temperatures matched towards the end of March 2007. When the temperatures at C1, C2 and C3 do not match, temperatures at C3 fall below the data recorded at traps C1 and C2. The rock and C4 temperatures stayed within 0.5 °C of each other, roughly showing the same ups and downs in recorded temperature (Figure 3-1d).

Lake temperatures at traps C1, C2 and C3 all begin to warm in the middle of June 2007. Temperatures at C4 begin to rise gradually on 3 June, joining the temperature trends of C1 through C3 on 8 June. Rock temperatures finally begin to rise on 10 July, but they never get quite as warm as the data collected from traps C1 through C4 (Figure 3.4e).

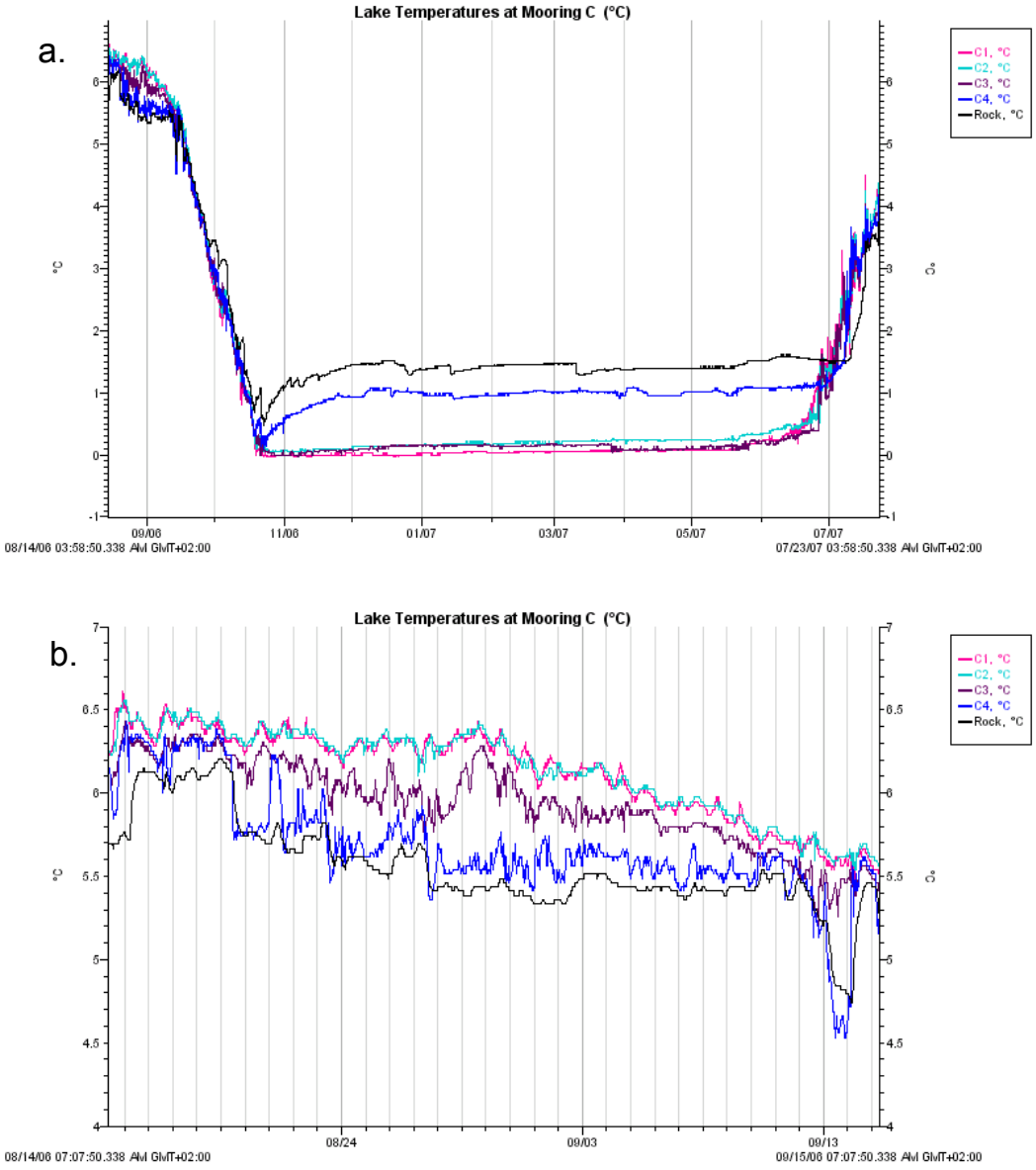

Figure 3.4a and b:
a.) Temperature data from Mooring C for the entire deployment period from August 2006 to July 2007.
b.) Lake Temperatures at Mooring C from 14 August to 15 September 2006, which show a short interval of thermal stratification.

c.

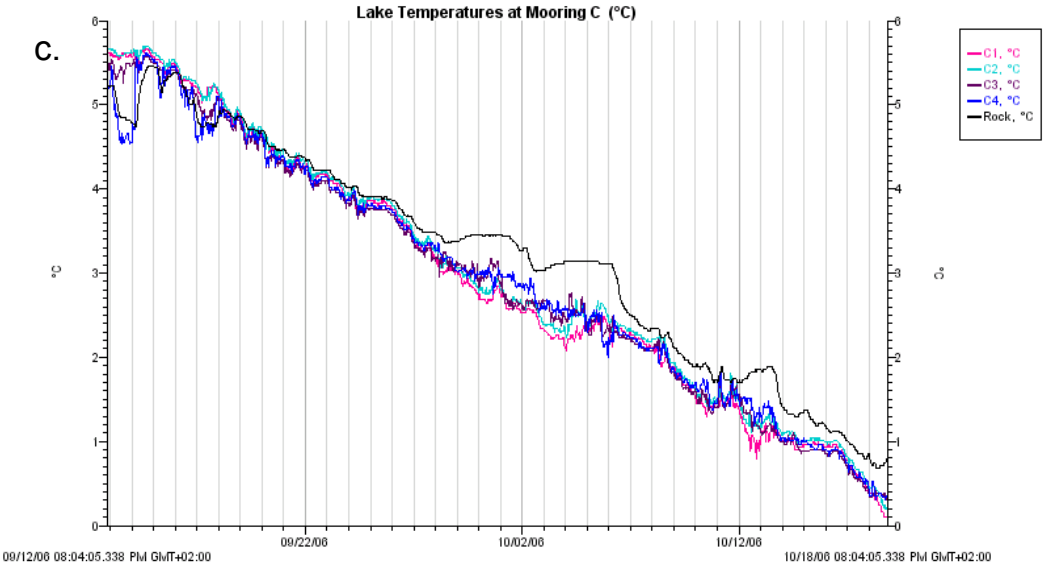

d.

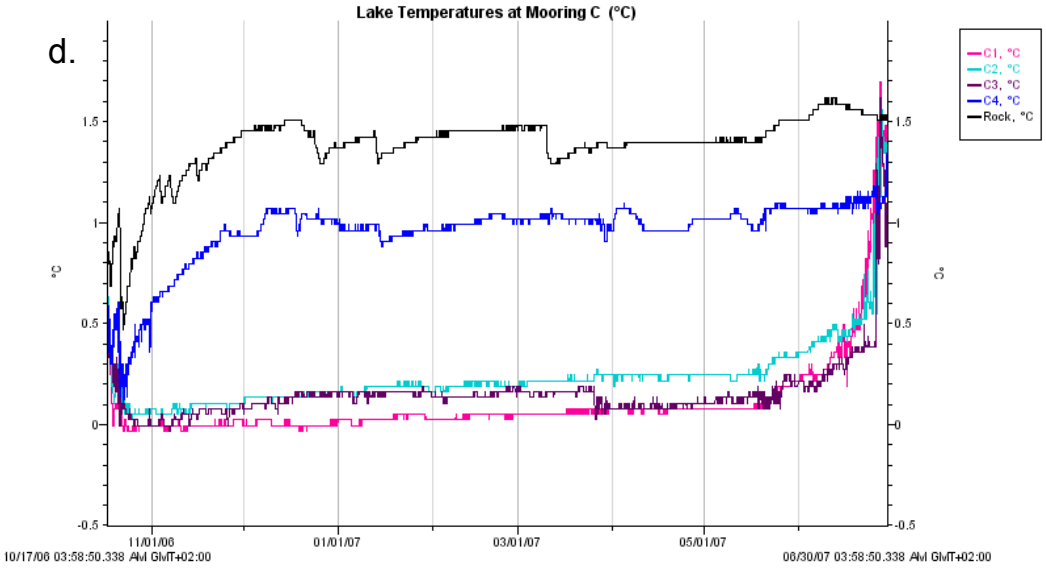

Figure 3.4c and d:
c.) Lake Temperatures trends of decline for the traps from 12 September to 18 October 2006.
d.) Lake Temperatures during the winter months from 17 October 2006 to 30 June 2007, note the predominant reverse stratification trends in the temperature data.

e.

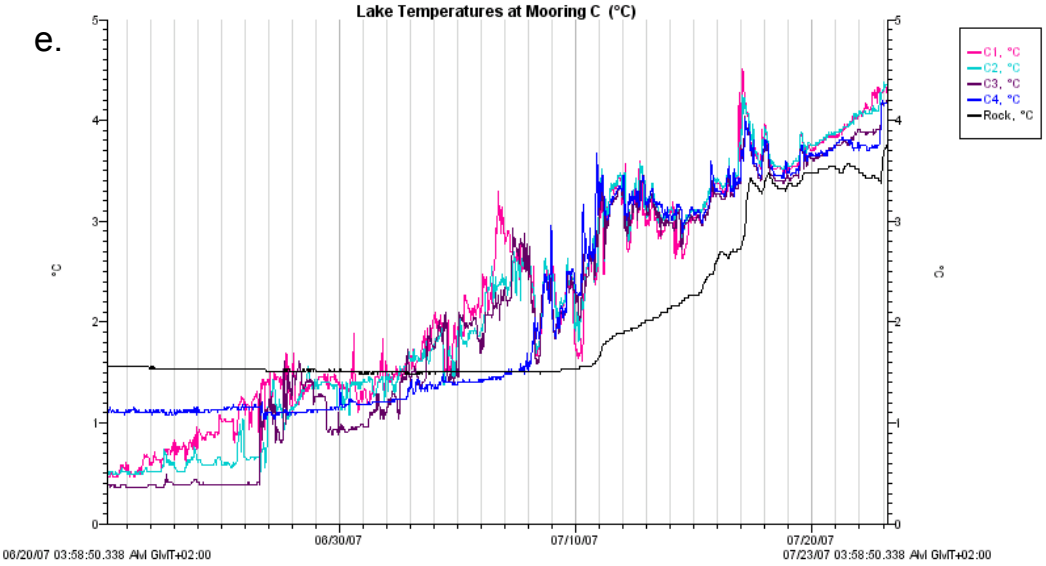

Figure 3.4e:
e.) Lake Temperatures, from 20 June to 23 July 2007, once Linnédalen enters the spring melt season.

III. Lake Bottom Water Turbidity

The temperature recorded by the Troll rose about 0.1°C from the day of deployment (16 May 2007) until the very early morning of 9 June 2007. During this time, no notable change occurred in the turbidity readings (Figure 3.5a). June 9th was the first day that temperature varied, rising from 1.260°C to 1.340°C and back down to 1.280°C. Mid 17th June was the first time turbidity was registered, with the highest NTU being 4.20 at 10:12pm, and fell by midnight of the 18th (Figure 3.5b). Interestingly, as turbidity rose, temperature fell (for the most part) over this interval (Figure 3.5b). Turbidity steadily rose until mid June 26th

(including a few small turbidity events) while temperature showed more variations. At 5:26pm on June 22nd lake temperature dropped to 1.070°C.

The first big turbidity event occurred in the mid afternoon on June 26th, when temperature began to increase about thirty minutes before turbidity increased. Within one hour, temperature increased by a little more than a degree, and turbidity rose to 18.4 NTU. For the next three days, the turbidity began an overall exponential decline, while temperature increased to one extreme, 2.68 °C, and fell to another, 1.56 °C, towards the end (Figure 3.5c).

The second, and larger, turbidity event occurred late at night on June 29th, and lasted until late June 30th. In slightly more than an hour, turbidity rose from 10.20 NTU to 90.00 NTU (Figure 3.5d). While the changes in turbidity were abrupt, temperature increased by less than half a degree initially and steadied out between 1.90°C and 2.00°C (Figure 3.5d).

For the remainder of the deployment period, there were smaller turbidity events, and an overall temperature rise of about 3.5°C. Even while the temperature had an overall rise, the temperature fluctuated as much as 2°C in a twenty-four hour period (Figure 3.5a).

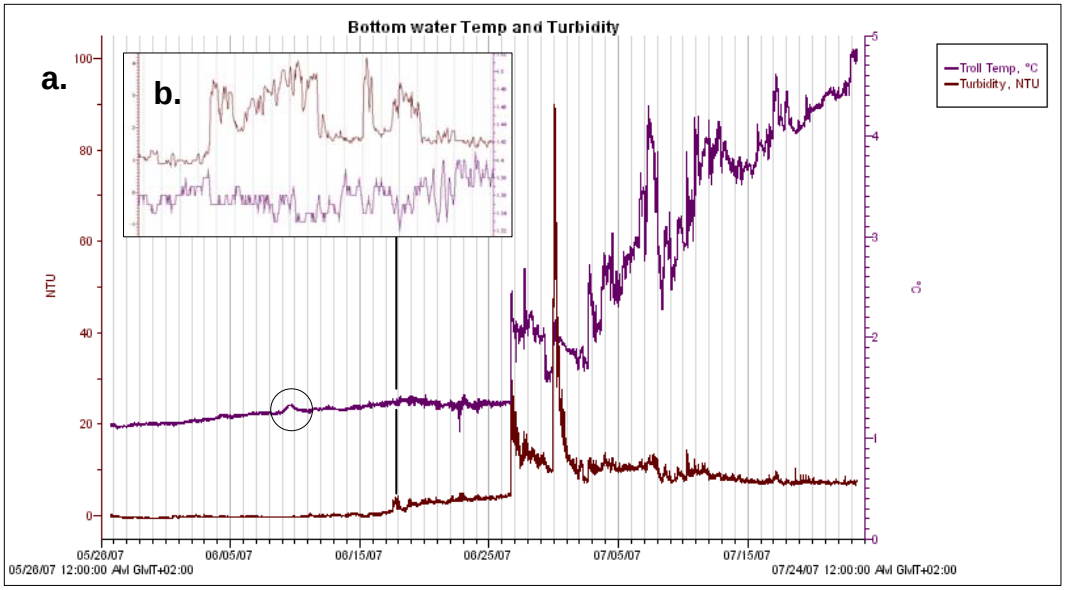

Figure 3.5a-b: Troll Temperature and Turbidity
a.) The temperature (°C) and turbidity (NTU) for the entire Troll deployment period. b.) The first notable increase in turbidity. Note the inverse relationship between temperature and Turbidity.

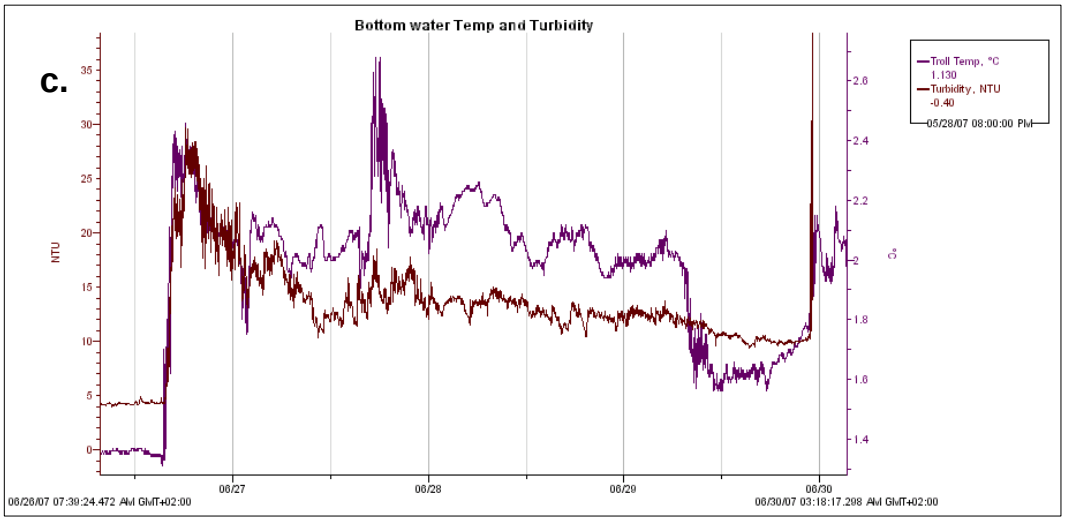

Figure 3.5c: The First Turbidity Event
Note how water temperature rose slightly before Turbidity increased.

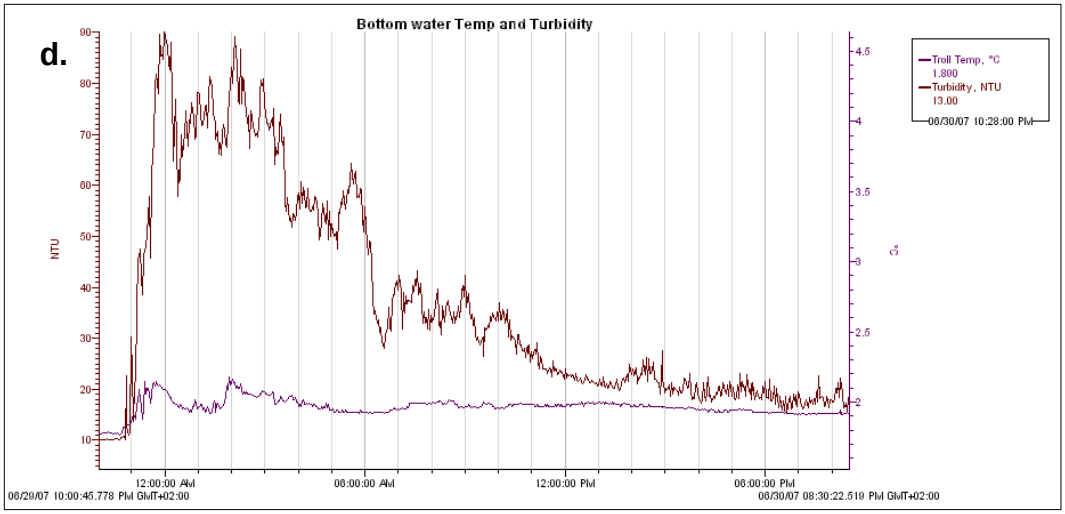

Figure 3.5d: The Second Turbidity Event
Note how temperature does not rise as drastically as seen in the first event.

IV. Meteorological Data

i. Air Temperature

Air temperature varies the most during the winter, when Svalbard does not receive sunlight, as a result of the advection of warm air masses associated with storm events. However, the temperatures stayed below freezing for the most part (Figure 3.6). Air temperature is less variable during the spring and summer, when the sun shines twenty-four hours a day, changing temperatures in the valley as the sun hits at different angles (Figure 3.6).

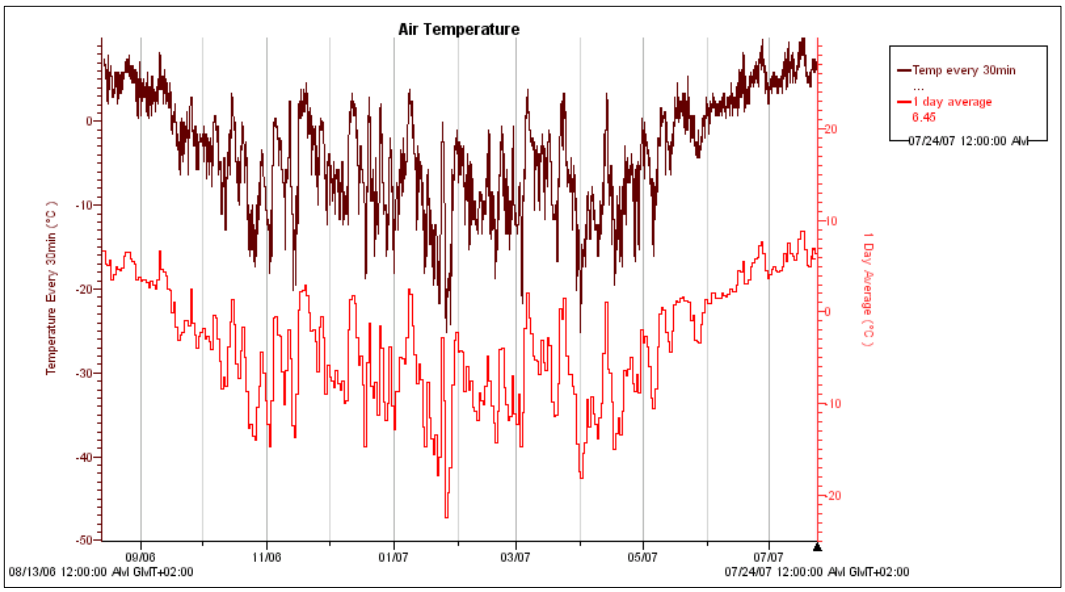

Figure 3.6: Air Temperature
Note how the temperature stabilizes during the spring and summer months. The maroon line is unaltered air temperature, and the pink line is a one day running average of the air temperature to visually simplify the information.

ii. Precipitation

Precipitation occurred fairly regularly throughout the year, except during the better part of February, when none fell (Figure 3.7a). Precipitation also did not fell on June 26th. Precipitation started to fall early on June 29th and continued until early evening. The second and the largest turbidity event began that night (Figure 3.5d and 3.7b).

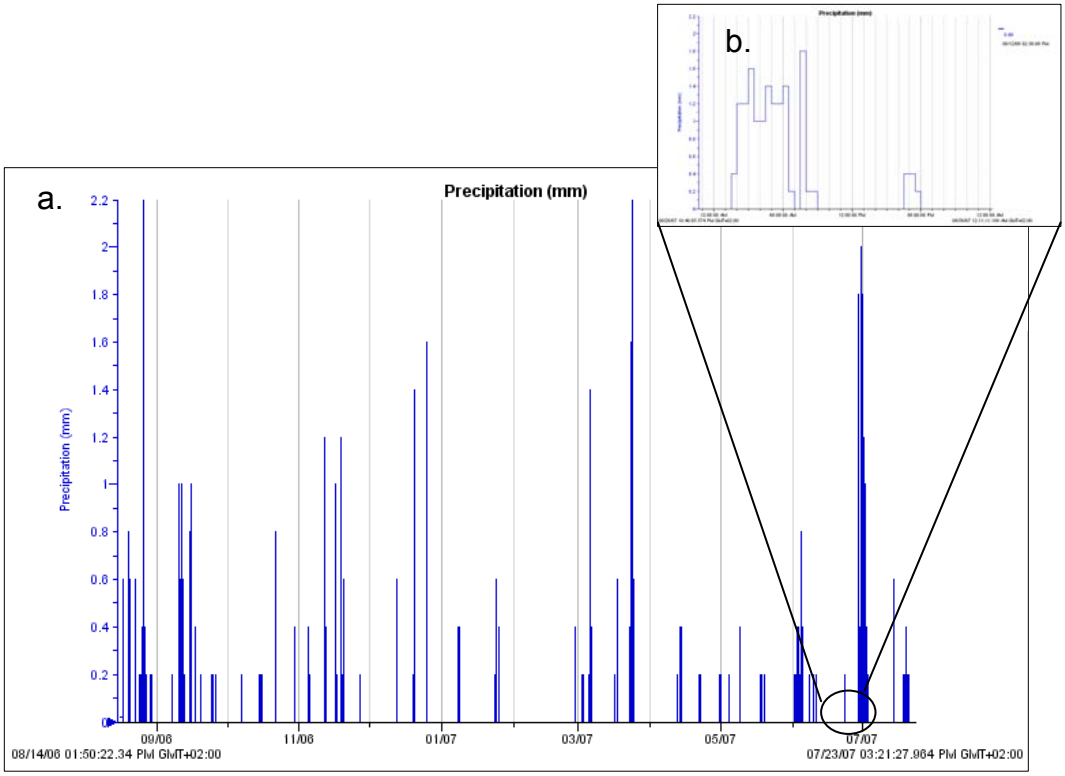

Figure 3.7 a-b: Precipitation
a.) Precipitation through the entire year (August 2006 to July 2007). b.) Precipitation on June 29th, during the largest turbidity event (see Figure 3.3d).

V. River Stage Temperature Data

During the spring and summer months the lower and upper stage temperatures follow each other very closely, usually within a half a degree or less (Figure 3.8a and b). The lower stage site is typically cooler than the mid stage site, but passes mid stage at peaks in temperatures (Figure 3.8b). During the winter, the lower stage site of the river stays much warmer than the mid stage, which reached ~5 °C twice (Figure 3.8a). The river froze up in mid September and thawed in late June. The two turbidity events recorded by the Troll followed a warming in both the lower and mid river stage temperatures (Figure 3.8c).

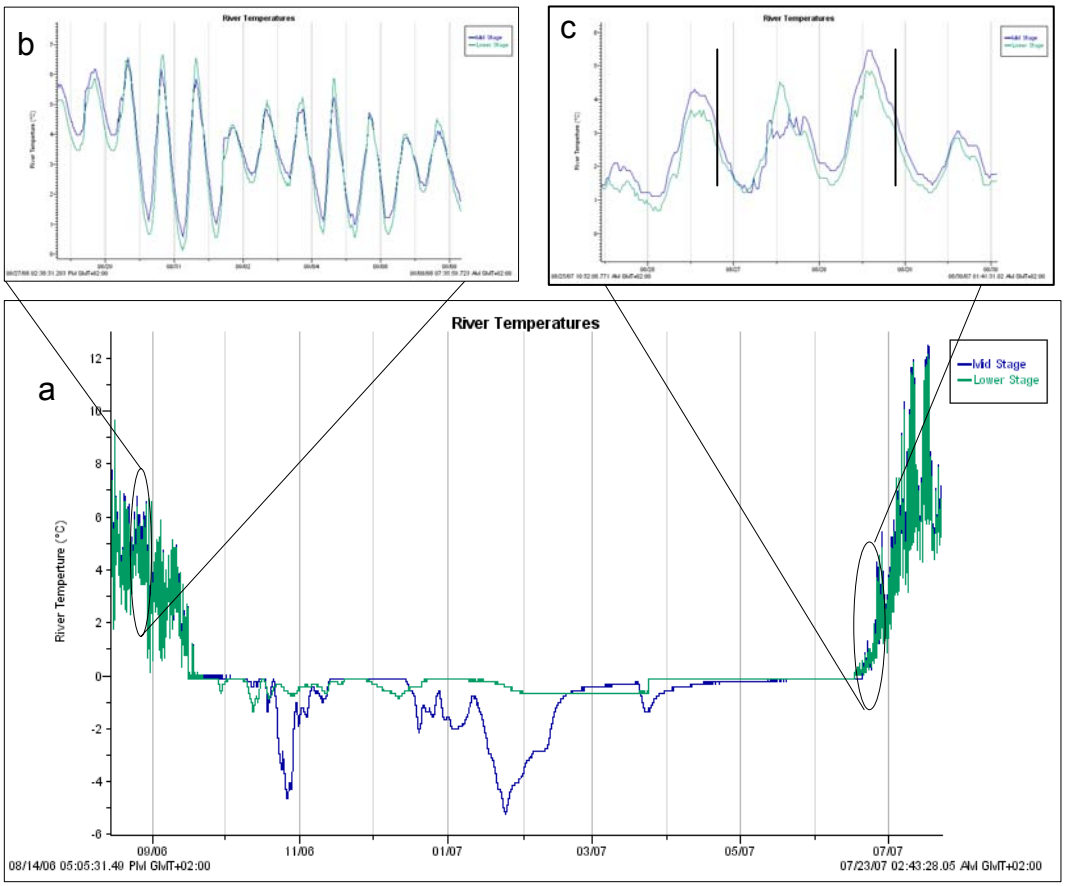

Figure 3.8: Mid and Lower River Stage Temperatures
a.) Mid and lower river stage temperatures for the whole year. b.) An enlarged portion of the graph showing how the lower stage typically is both cooler, and how it can be warmer than the mid stage at peaks in temperatures. c.) An enlarge portion of the graph, with vertical black lines approximating the timing of the two turbidity events.

VI. Snow-Tree Temperature Data

Rungs 2-4, at 15, 30 and 45 cm respectively, record the same temperature until rung 2 pulls away on October 8th, and eventually records consistently warmer temperatures than rungs 3 and 4 on October 13th (Figure 3.9b). Rungs 3 and 4 begin recording different temperatures on October 13th (Figure 3.9b). For the duration of the winter, the rungs are reversely stratified (as a result of insulation created by snow depth), with rung 1, at 7 cm, recording the warmest

temperature, and rung 4 recording the coldest (Figure 3.9a). From late May 21st, all four rungs record -0.101 °C through June 25th, at which point rung 4 begins to record warming temperatures (Figure 3.9a and c). Rung 3 begins to record warmer temperatures early morning on June 26th, with rung 2 starting by early afternoon (Figure 3.9c). Rung 1 does not begin to record warming temperatures until June 28th (Figure 3.9c).

The light intensity measured at each rung followed a pattern very similar to the temperatures recorded at each rung, except that there is no variation in luminosity during the winter (Figure 3.10a). Rung 1 stopped recording light first on October 9th, rung 2 followed on October 13th, rung 3 stopped on the 16th, and rung 4 on the 17th (Figure 3.10b). Rung 4 begins to record light again on June 23rd, rung 3 on June 25th, rung 2 on June 26th and rung 1 finally records sunlight on June 27th (Figure 3.10c).

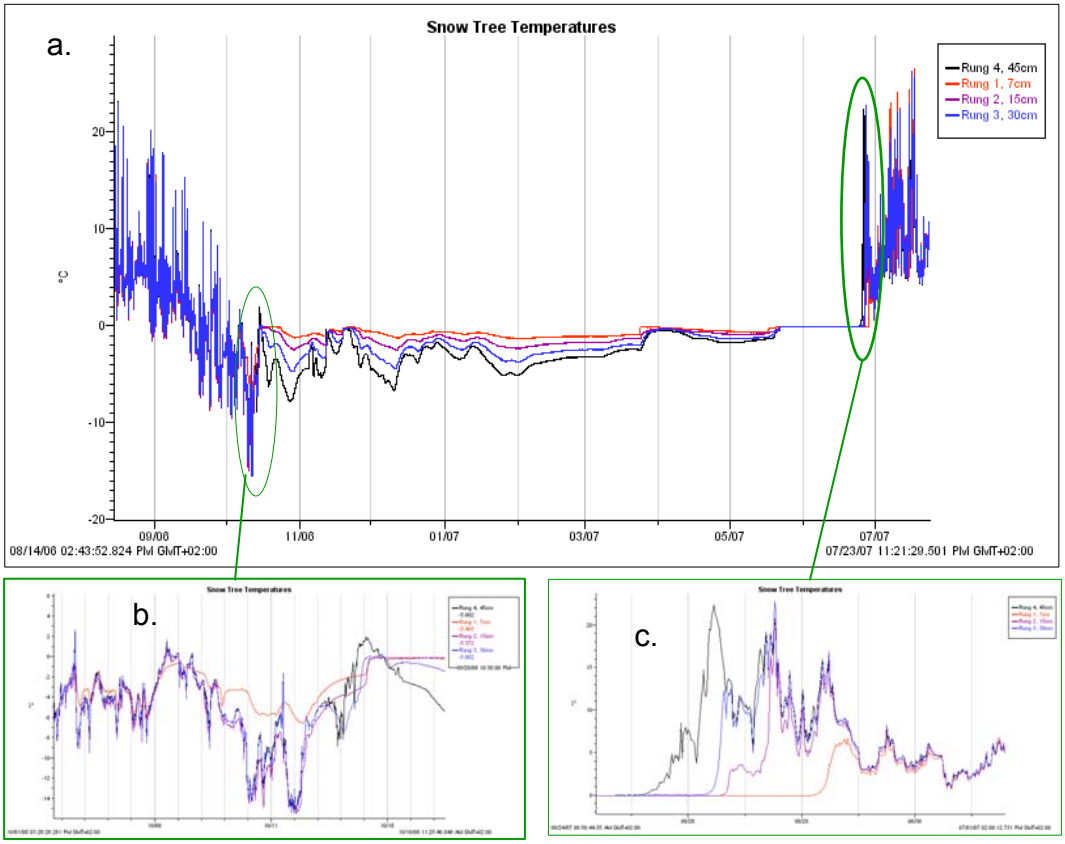

Figure 3.9: Snow Tree Temperatures
a.) Temperatures at all four rungs for the deployment period. b.) An enlarged portion of the graph showing the temperatures at each rung as snow accumulates around the tree. c.) An enlarged portion of the graph showing the temperatures at each rung as the snow melts.

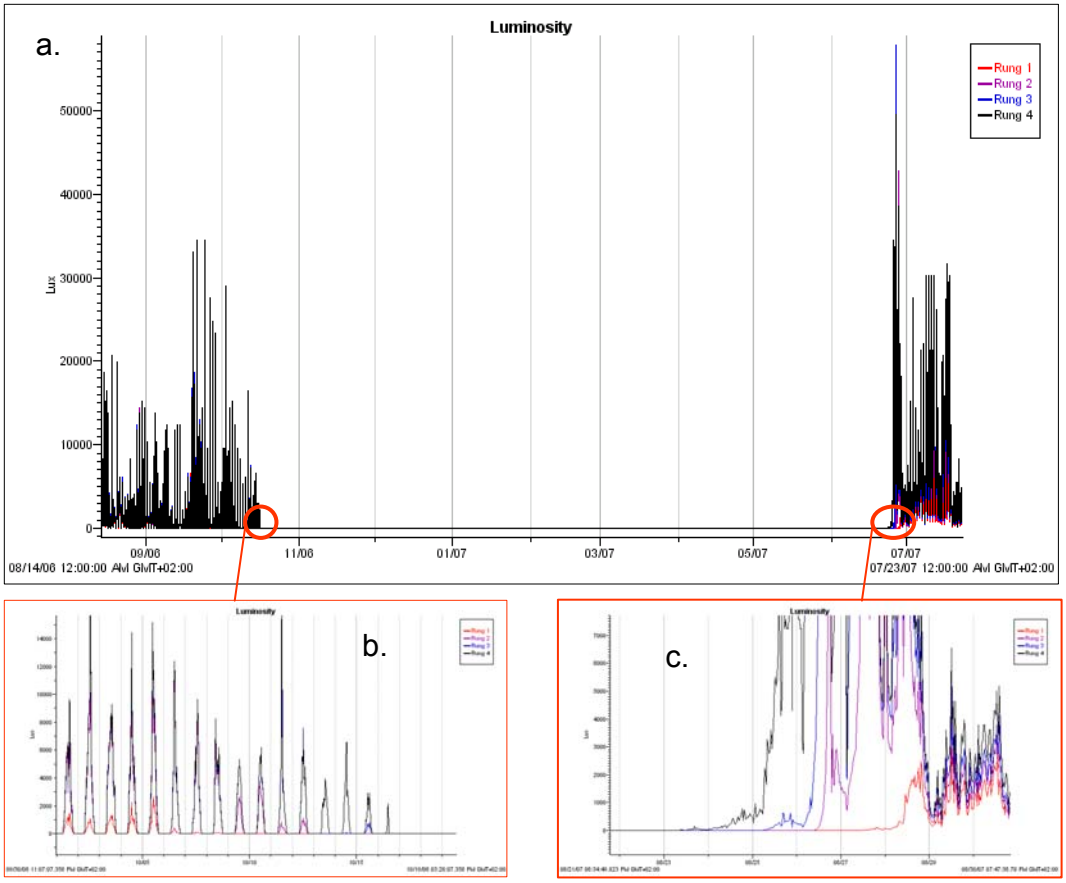

Figure 3.10: Snow Tree Light Intensity
a.) Luminosity at all four rungs for the deployment period. b.) An enlarged portion of the graph showing light intensity at each rung as they are covered by snow. c.) An enlarged portion of the graph showing light intensity at each rung as the snow melts.

VII. Automated Camera

The plume camera captured the loss of snow cover during the spring, and the thawing of the inflow stream and Linnévatnet. A few key photographs show this progression (Figure 3.11).

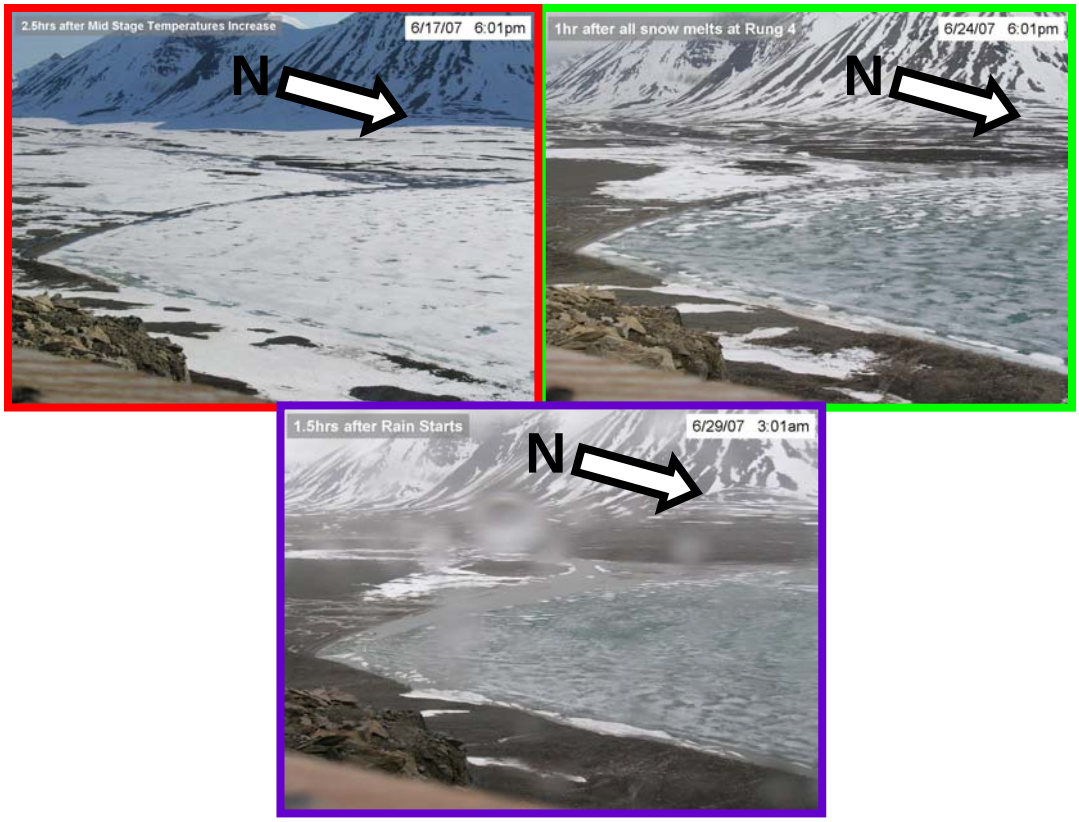

Figure 3.11: Key Plume Camera Photographs
The first photograph is shortly after mid-stage thaws. The second is shortly after rung 4 is uncovered. And the last is shortly after the rain event preceding the largest turbidity event. Note the loss in ice coverage and snow over time.

VIII. Lake Level

The water level in Linnévatnet declined slightly for the first few days after the levellogger was deployed, and began to rise steeply on June 3rd (Figure 3.12a). An overall decline in lake level began on June 10th (Figure 3.12a). During this overall decline lake level did rise briefly, though never reaching the levels observed from June 3rd to the 10th (Figure 3.12a).

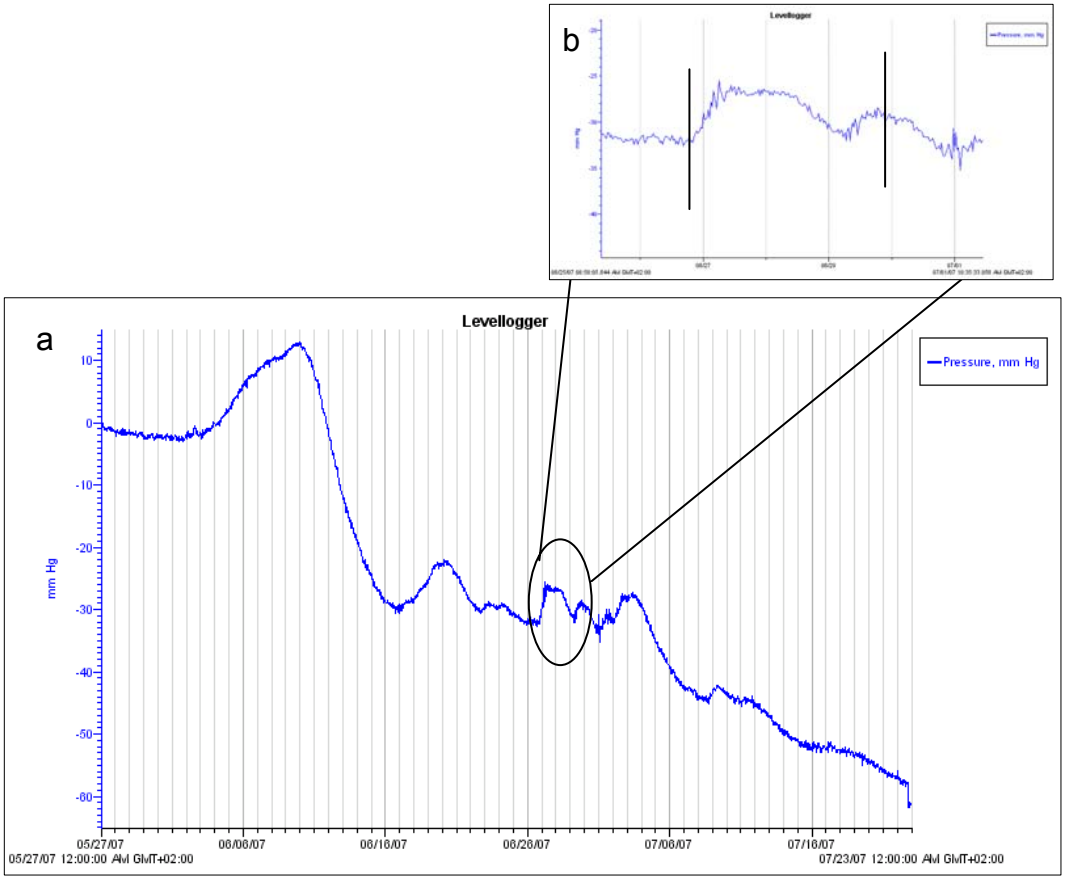

Figure 3.12a-b: Levelogger
a.) Pressure recorded by the Levelogger during deployment. b.) Enlarged portion of the graph with vertical black lines marking the peak timing of the two turbidity events.

Chapter 4:

Interpretations and Discussion

I. Sediment Traps

For traps C1, C2, C3 and C4, both the amount of sediment deposited in centimeters and the sediment flux increased in the deeper traps (Figure 4.1 and Table 3.3). Further, the mean grain sizes in each trap were shown to become successively coarser (Figure 4.1). During the 2004-2005 deployment period, sediment flux followed the same increase, but for the deployment period 2005-2006 sediment flux increased through trap C3 only to decrease at trap C4 (Table 4.1).[37]

	Sediment Flux (g/cm2)		
Trap	Yr 04-05	Yr 05-06	Yr 06-07
C1	0.027	0.240	0.106
C2	0.128	0.310	0.257
C3	0.159	0.320	0.329
C4	0.251	0.299	0.463

Table 4.1: Sediment Fluxes for Mooring for the past three deployment periods.

The differences in sediment fluxes from year to year attests to how variable sedimentation in Linnédalen is year to year. The valley does not warm in the same way every year, nor do rain events occur at the same time every year. This variability of environmental factors changes what and how much of different grain sizes are deposited each year.

With that said, despite differences in sediment fluxes from year to year, the overall patterns of grain size increases and decreases are remarkably similar (Figure 4.2). The mean grain size graph for C4 from 2005-2006 increases in the

middle portion, and is preceded and followed by finer grains sizes, as seen in C4 from 2006-2007.

[37] Roop, 2007 and McKay 2006.

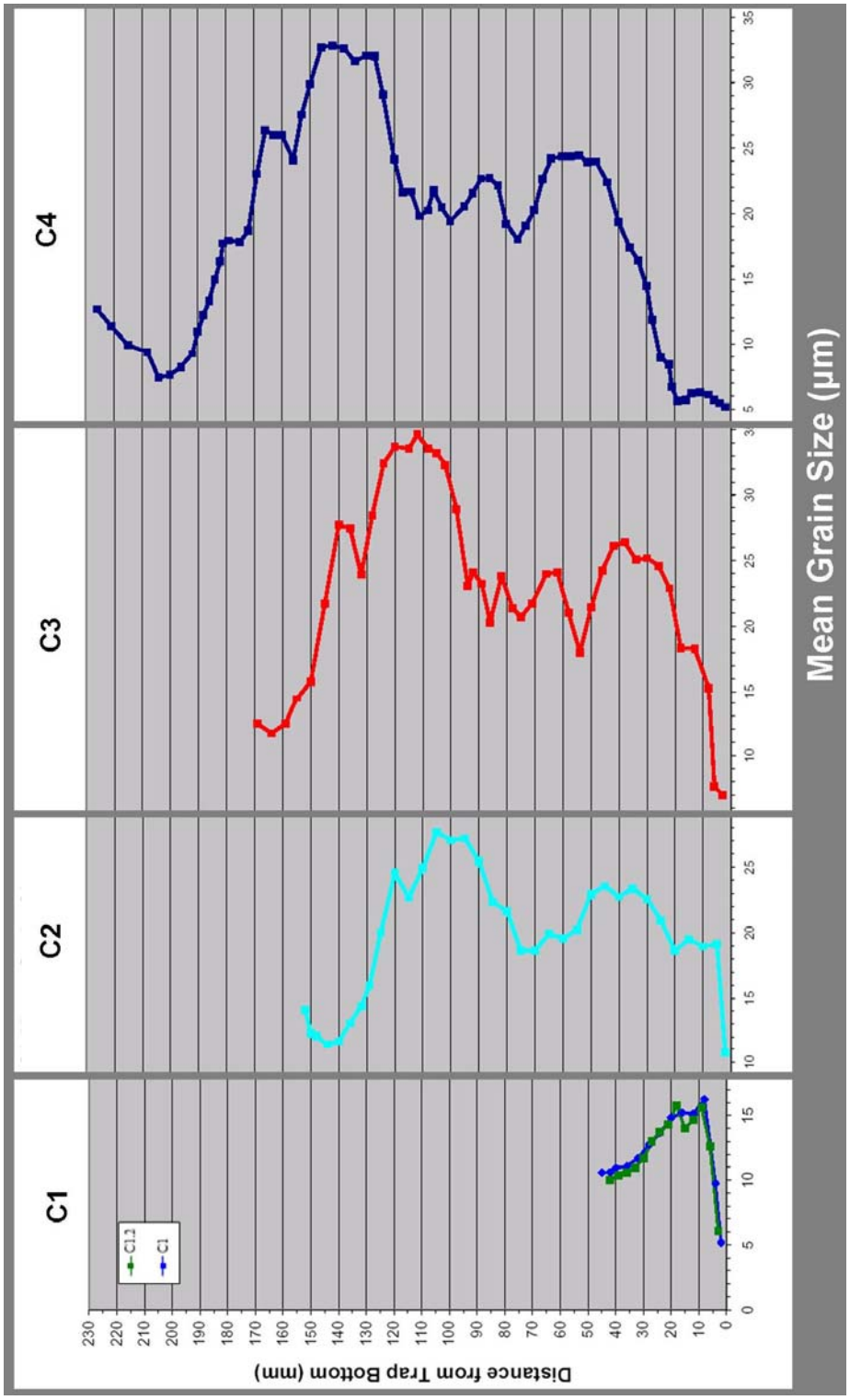

Figure 4.1: Yearlong Mooring C
Note increase in amount of sediment in each deeper trap, as well as coarser grain sizes.

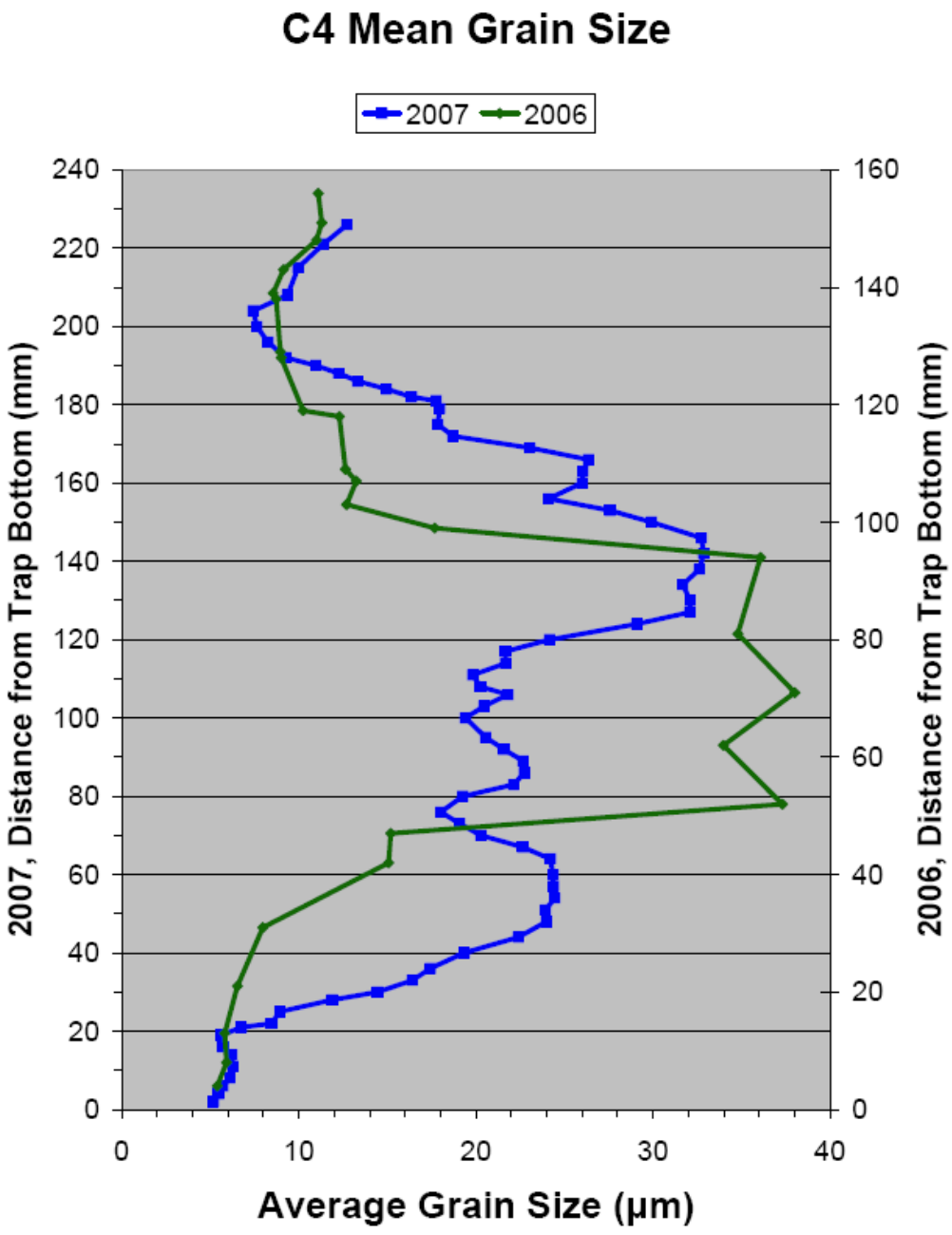

Figure 4.2: Trap C4 for years 2005-2006 (green) and 2006-2007 (blue). Note different scale on primary and secondary y-axis.

Both the yearly and the spring traps at Mooring C show at least two coarsening events (Figure 4.1 and 4.3). All traps except C1, C1.2 and Cs show more than two coarsening events. Even the coke bottle traps, where the peaks are less defined by data points, have three coarsening events.

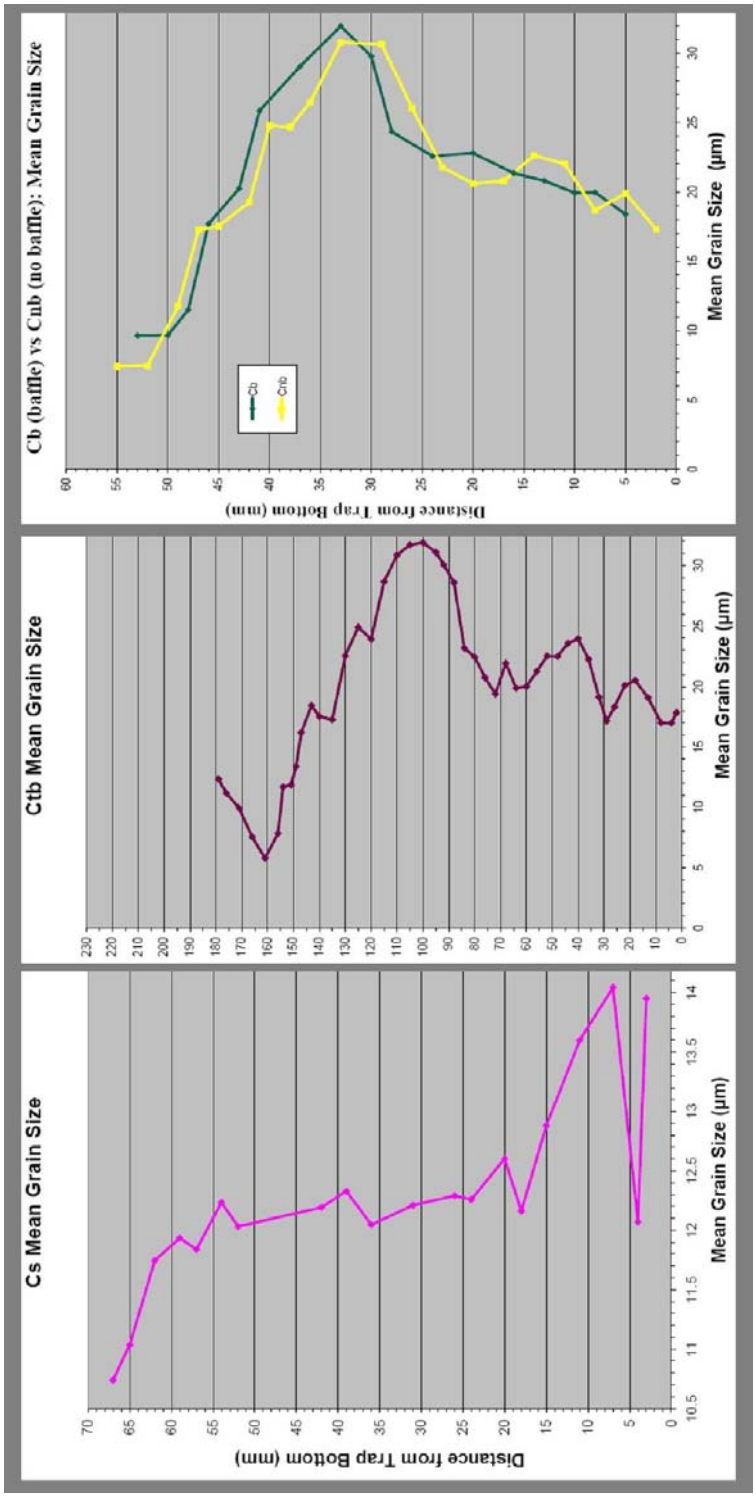

Figure 4.3:
Spring trap correlation.

Trap Cs does not appear have two coarsening events, but this may be a result of incomplete sampling. The first three mean grain sizes, at the bottom, start at 13.6μm, decrease to 12.1μm, and then increases to 14.0μm. This change in grain sizes might result from one of two things. First, the sampling thickness, 1mm, of the second Cs data point sample could have artificially made it appear that grain size dropped. Had the trap been sampled at different intervals the graph may have looked different. For example, the grain size changes could have been smoother. Even so, the sub-samples intervals chosen for Cs respected noticeable differences in visual and X-ray stratigraphy. This technique was applied to all the other traps (except C1.2), which showed no such discrepancy.

Further, when compared to C1, the increase in grain sizes is logical. Trap Cbt does not have finer sediment at the bottom of the trap like its yearlong counterpart, C4. Likewise, trap Cs was deployed at the same time as Cbt, and does not contain the finer sediment present at the base of C1. The first three samples in Cs mimic the rise and fall from the first coarsening peak in C1 to its second, suggesting that we only see the grain size decrease from the first coarsening event in trap C1.

On Mooring C, each successively deeper trap contained more sediment. The more sediment, the more closely the grain sizes in each trap follow the coarsening and fining in the other traps, especially for traps C3, C4 and Cbt, with C2 following a little less closely (Figure 4.2). Previous studies have discussed the possibility of water flowing into Linné, which has a specific temperature and

density, seeking the depth in the lake whose temperature and density most closely match those of the inflow water, creating interflows. [38] Flowing in at a specific depth would carry any sediment load to that depth and rain sediment to deeper depths, effectively changing the signal each trap records in grain sizes. Therefore, in the case of dominant interflows, the grain size patterns at mooring C would not be expected to so closely reflect each other. Although this may have occurred in previous years, during the 2007 sedimentation year, because of the similarity of the particle size at the mooring C traps, underflow or interflow sedimentation does not appear to be common. Rather, this similarity suggests that most of the sediment was distributed by overflow or homopycnal flow. If the deposited sediment in each trap resulted from independent interflows reaching only specific traps, the resulting graphs would not be so closely correlated.

One exception to this might be the grain sizes from trap C1. Considering the lack of sediment in C1, I may not have been able to sub sample small enough to capture all the changes in grain sizes. On the other hand, for all that the other traps mimicked one another in grain size patterns, and that C1 did have two coarsening peaks, there may have been an interflow to the point that it did not deposit sediment in the first trap. Turbidity events could have acted as interflows, excluding C1 in some events. Especially as the valley began to warm and the deeper water depths remained warmer than the surface temperatures, the incoming water temperatures were closer in temperature to the bottom

[38] Roop, 2007 and McKay 2006.

temperatures, causing the incoming water to drop below the level of C1. Even so, overall, the lake temperatures remained similar enough to each other, and the incoming water, so no one trap (besides C1) diverted from the overall patterns present in the mooring C traps.

Due to the simplification of grain size patterns present in trap C1, it is hard to correlate what was deposited in C1 to the other mooring C traps, beyond noting that all the yearlong traps were deployed and collected at the same time. Besides that, because the patterns in between C1 and the other traps diverged, it is hard to say this coarsening peak in C1 was deposited at the same time as this peak in such and such a trap without knowing the timing of deposition in each trap. There is no way to know which coarsening event, present in the deeper traps, did not get recorded in trap C1. The two peaks in C1 could be correlated to the first and third or second and third, respectively, in the deeper traps. But with that said, the other traps can be compared to one another by event, because they all record each rise and fall to some extent.

Traps C2, C3 and C4 each have the same rises and falls, except between the two coarsest peaks in C2, where one of the peaks is missing (Figure 4.2). Whether this difference is due to sampling differences or represents localized sediment distribution events is not known. Determining which of the peaks is missing is not possible. But because the two coarsest peaks in C2 can be correlated to the two coarsest peaks in the other traps, sediment deposition in trap C2 can be constrained to some degree.

Traps C4 and Cbt collected sediment at the same depth, but were not in the exact position spatially (their moorings were within 10m of each other). Generally speaking, the grain sizes in each graph mimicked each other, but where the first peak in C4 is coarser than its second, the opposite is true for Cbt. That is not to say that these peaks therefore represent different events. But rather they will not necessarily record the same grain sizes for the same event, because their moorings are not quite in the same location, meaning that the year-long and spring mooring at location C are not right on top of each other. The subtle differences in sediment distribution within the basin could reflect the spatial differences in grain sizes in an inflow plume. By being in a slightly different spot, each trap is recording a slightly different part of a turbidity event. For the first event in each trap, the yearlong mooring could have been located towards the center of the plume, where higher velocities can carry larger grain sizes, because the grain sizes in the first peak in Cbt is finer than those in C4. The reverse could be true for the second turbidity event in each trap, where if the spring mooring were located in the faster moving part of the plume, it would explain it having coarser grain sizes at that peak compared to C4.

Besides that inversion between the first two coarsening events in C4 and Cbt, the grains sizes in each trap follow each other, except for the beginning of trap Cbt. Cbt does not contain the finer sediment present in C4. A difference explained by Cbt being deployed so much later that C4. Cbt was not in the lake when it froze over for the winter, slowing the water down, allowing the very fine

sediment to deposit. Rather, Cbt starts off with a coarser grain size, before decreasing for two sub samples only to rise to the first coarsening peak correlated to the first peak in C4.

Trap Cs also showed an initial coarse grain size before dropping, only to rise again, which could be explained by sample spacing or that only parts of turbidity events represented in C1 is present in Cs. But when the initial coarse grain size in Cs is considered with the initial grain size in Cbt, these grain sizes may not result from any turbidity event. Rather, the spring traps were deployed after the much finer sediment had a chance to settle because the lake was covered in ice, and the inflow was frozen to its streambed. In other words, the spring mooring was deployed in the absence of any current in the lake. When moorings are deployed, no matter how carefully, sediment will be kicked up to some degree. During the summer, when the yearly moorings are deployed, any sediment remobilized during mooring deployment would likely be carried further into the lake basin before it becomes trapped in the funnels. But during the winter, in the absence of currents, any sediment re-suspended from trap deployment could become trapped in the funnels. This phenomenon may explain the coarser grain sizes found initially at the bottom of trap Cbt; however, it is arguable that the plume from deployment would not extend 12.5m up to reach trap Cs. But the initial grain size in Cs is finer than those found in Cbt, a pattern of fining upwards that would be expected should the traps be recording sediment from the deployment plume.

i. Modified Spring Traps

Modified spring traps were deployed to evaluate the efficiency of the currently used traps designs, the so-called traditional traps for both the spring and yearlong. The coke bottle funnel traps, with and without a baffle, show the three large coarsening events evident in traps C2, C3, C4 and Cbt, though Cb and Cnb record the three peaks to a less exaggerated extent. The changes in grain sizes are less distinct in the coke bottle traps as a result of the increased receiving tube diameters, compared to their inclined funnel counterparts. The opening of the coke bottle required larger receiving tubes, which meant that the same sampling technique used on the other traps translates to a lower sample interval for the modified traps. The traps could only be sampled at so small an interval, resulting in grain size peaks that were less noticeable. Each sample had more sediment in it, diluting the grain size, and thus, homogenizing the grain sizes for the whole trap.

Neither Cb nor Cnb showed the coarser grain size at the bottom of the trap like Cbt and Cs did, which was possibly a result of the sampling interval and the resulting dilution of the grain sizes. Alternatively, it is possible that the coke bottle traps just did not record the deployment plume. But then why would Cbt show it?

The ability to evaluate the effect of the baffle on sediment trap efficiency is likewise limited, as a result of the larger receiving tube diameter and resulting stratigraphic resolution. In general, the baffle seemed to make the collected sediment more homogenous. Trap Cnb has a wider range of grain sizes, though

each coarse peak, in Cb and Cnb, is very close in grain size, if not the same. The muted look of Cb could result from how the trap was sampled, but both Cb and Cnb were sampled following visual and X-ray stratigraphy exceptionally closely, to ensure a clean comparison. Even with the slight differences, the overall message is the same. There were three main coarsening events, thus turbidity events.

Again comparing Cb, as a result of the large receiving tube, with Cbt and C4 effectively is not possible, beyond noting that they all show three coarsening events. There remain too many differences between the grain size results from the traditional spring traps and modified spring traps to make any further correlations. Even if the small intricacies observed in Cbt and C4 were actually captured and recorded by Cb, the way Cb was sub sampled glossed over the finer details, not allowing for any further speculation. Thus, any definitive conclusion on trap efficiency, whether inclined funnels are truly superior to straight walls, was not possible.

ii. Sampling Technique

Both halves of C1 were sub sampled in attempts to evaluate the impact of sampling the receiving tubes in different ways. For this experiment, subsamples were collected 1) at uniform sample interval (irrespective of stratigraphic contacts), and 2) using the visual and X-ray stratigraphic boundaries to guide sampling. For as much as there were variations between C1 and C1.2, they were slight, leaving the earlier conclusions intact. There is not a significant difference

between sub sampling according to stratigraphy and X-ray, versus sampling at regular intervals. However, had I sub sampled C1.2 at slight larger intervals, the stratigraphic units would be less distinct, much in the way the coke bottle traps were with their larger receiving tubes. As long as the sub sampling intervals are small enough, the overall signal of the particle size data will be documented and sampling need not be guided by visual or X-ray stratigraphies.

II. Logger Data and timing of Environmental Events

The ultimate goal of this research is to understand how various environmental conditions are expressed in the yearly sediment deposited in Lake Linné. Once these relationships are better understood, it should be possible to interpret past environmental conditions.

The timing of the events in the valley, as things started to melt and move, is important in understanding the turbidity events and the pictures from the plume camera, showing events in real time (Table 4.2 and Figure 4.4).

Turbidity Event	One	Two	Three
	June 17, 1:14pm	June 26, 3:30pm	June 29, 10:48pm
Lower River Stage	June 17, 4:00am		
Mid River Stage	June 20, 1:00pm		
Snow Tree Rung 4		June 24, 5:30pm	
Snow Tree Rung 1		June 28, 5:00am	
Rain			June 29, 1:30am-6:00pm

Table 4.2: Timing of Environmental Conditions in Linnédalen.

About nine hours after the lower stage site of the river began to flow, experiencing diurnal temperature fluctuations, the first turbidity event was recorded in the lake. The mid stage of the river began to flow three days later, indicating the river was continuing to thaw in a delayed manner upstream. As

other events were occurring in the valley, the river continued to thaw up towards the glacier. However, in the absence of more loggers upstream, confining the timing of complete de-thawing of the inflow stream is not possible.

As the river continued to thaw upstream (beyond the thawing of the mid stage river logger, the timing of which is not known) rung four of the snow tree became free of snow two days before the second turbidity event occurred. Rung 1 became free of snow two days after the second turbidity event began. Sometime between rungs 4 and 1 becoming free of snow, the snowmelt in the valley, along with the continuing thawing river, influenced the occurrence of the second turbidity event. More importantly, during this period the snow tree became completely free of snow in just for days. Such a quick period of melting at the snow indicates that a major event is likely happening in the valley, the spring melt.

The third turbidity event, by far the largest, is likely a combination of many factors occurring simultaneously in the valley. By this point the river is probably completely thawed, and most of the snow has melted off the valley bottom. The plume camera confirms this and also indicates that significant snow cover still remained on the higher elevations. Although the snowmelt at the snow tree arguably represented conditions possibly relevant only to that location, snow coverage, shortly after the rain starts, is noticeably less. With a thawed river, and very little impeding snow cover, a rain event has a much higher potential to mobilize sediment that the melting snow (turbidity event 2) did not have the power to transport previously.

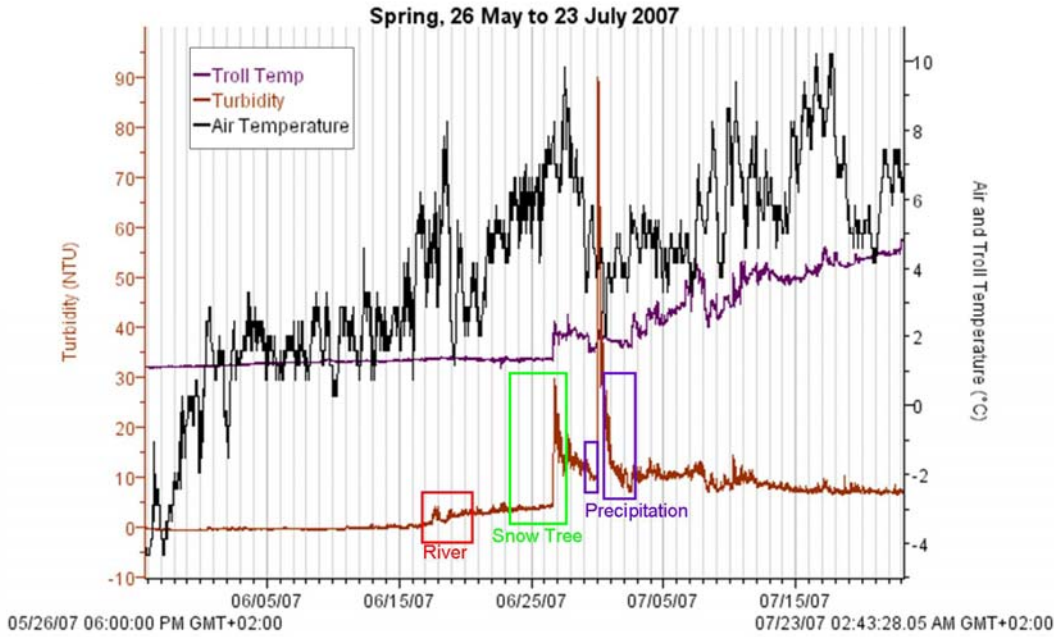

Figure 4.4: Timing of Environmental Conditions

III. Correlating the Logger and Trap Data

The Troll and the spring traps were deployed on May 26, 2007. Sediment collected in the spring traps was therefore deposited during the same time that the Troll made its measurements. Being deployed at the same time constrains when the three main coarsening events recorded in all the deeper traps occurred. We know that they occurred after the finer sediment settled out of the lake over winter, supported by the finer sediment in the bottom of C4 and subsequently absent in Cbt (Figure 4.5).

The first and smallest turbidity event began shortly after the lower site of the river began to flow, supplying the lake with the first new sediment of the season. In all the yearlong traps, the first coarse peak (and the second largest)

occurs at the same time that the river starts to thaw and flow. As the river continues to melt upstream, and the snow begins to melt around the snow tree, another turbidity event is recorded by the troll, while the traps record another spike in grain size between the two coarsest peaks. Finally, as most of the system is thawed and a rain event occurs, the Troll records the highest turbidity of the season, and the traps show their coarsest grain sizes.

If the coarsest peak in the traps is correlated to the largest turbidity event, the remaining turbidities measured never surpass the values of the second two events. Because no notable events occur in the valley other than rain, which doesn't seem to increase sediment influx (Figure 4.5), the increase in sediment size at the top of the traps has to result from something else. At this point they are probably recording glacier ablation, because all the other noise, such as environmental conditions that had been occurring, has stopped.

It is important to note that the Troll measures turbidity in terms of water opacity and that particle size can also influence the measured turbidity. As particle size decreases, the effective opacity increases – even though sediment concentration may remain the same. The particle size increase at the top of the traps therefore may represent an influx of coarser textures that is not recorded as an increase in turbidity. In all likelihood, this sediment was deposited over a longer period of time and in much lower concentrations, and thus was not recorded as any significant turbidity event. As more and more of the glacier melted, giving more force to the inflow stream, and thus, the ability to carry

coarser and coarser sediment, the increasing grain size records the glacier ablation for the season.

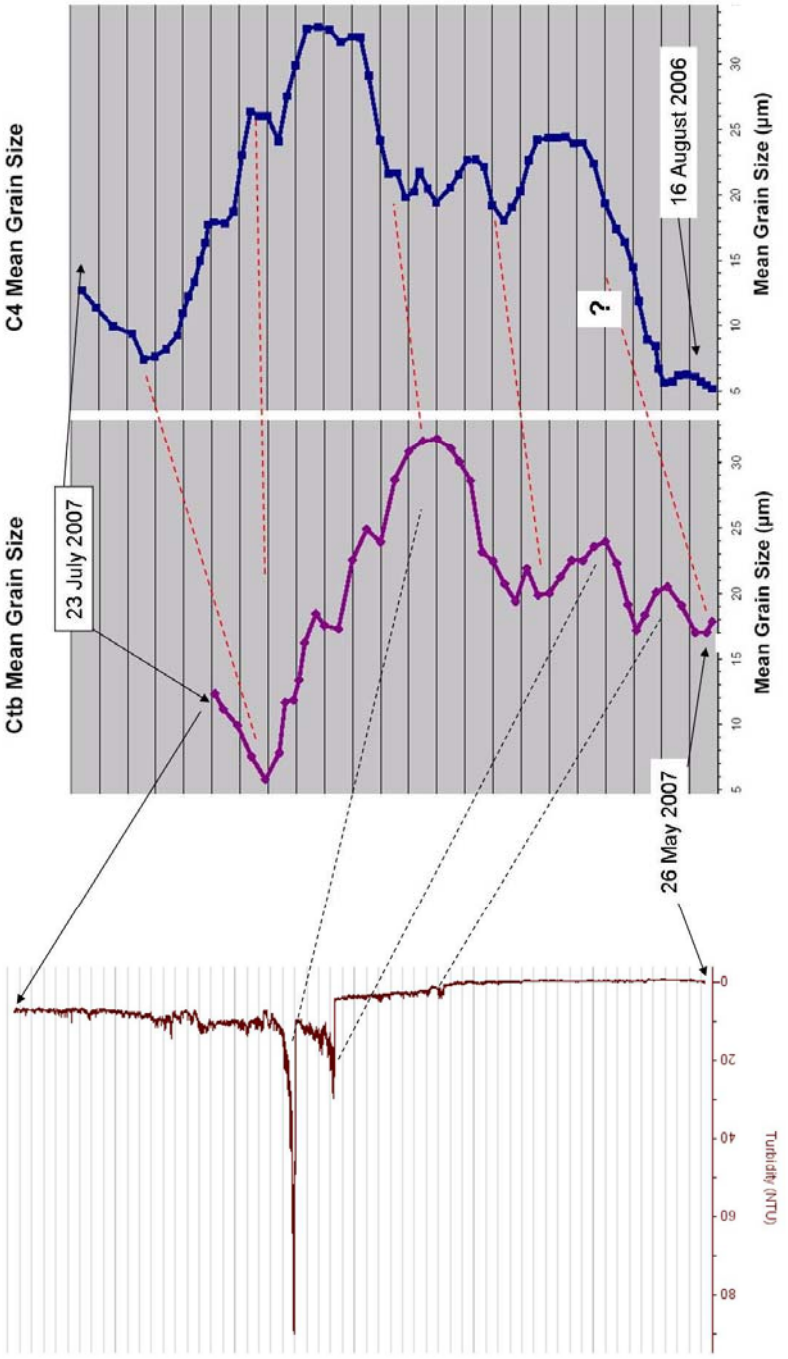

Figure 4.5: Turbidity, C4 and Cbt Correlation.

IV. Year to Year Sedimentation

Understanding which signals in the traps correlate to what environmental conditions is the first step to better understanding the varves in Linnévatnet. This study used collected sediment in traps and measured environmental conditions in the valley to understand the significance of grain size variations. But to confidently correlate grain sizes in the varves to what environmental conditions deposited the sediment, and in the long term to discuss climate change, we need to understand what the sediment we collected and evaluated will look like as a varve.

To better quantify what this year, 2006-2007, would look as a varve it helps to graph C4 from 2005-2006 with this year's C4 trap data. C4 from 2005-2006 had less sediment, but more variation between fine and coarse grain sizes than 2006-2007. The resulting varve for 2005-2006 would be smaller, but the difference between the clay and silt layer would be more distinct. While this year's varve would be larger it might be less distinct. Potentially allowing for mistakes to be made when silt and clay layers are determined to be part of what varve couplet, if the possible environmental conditions from year to year are poorly understood.

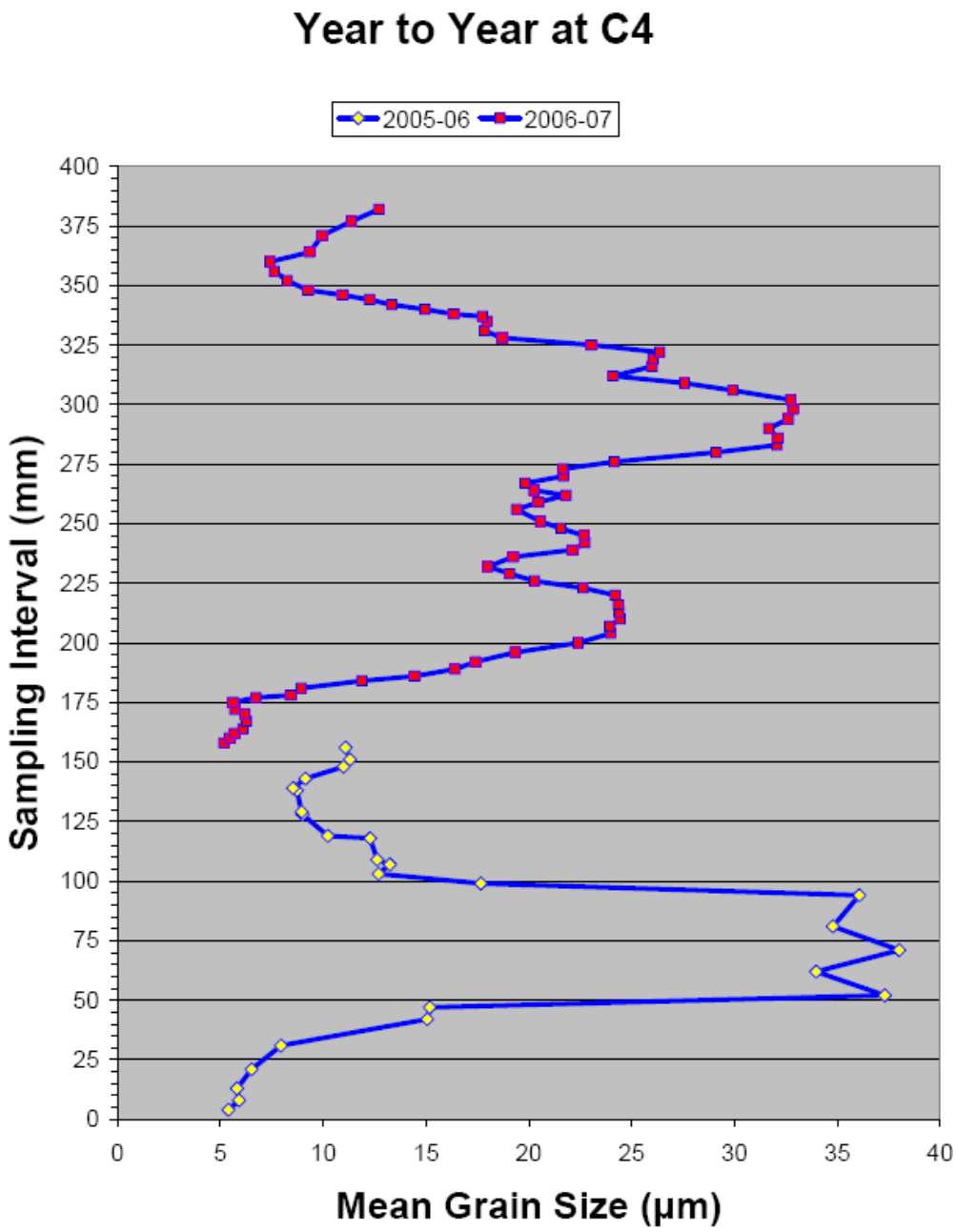

Figure 4.6: Comparison of 2006 and 2007 Sedimentation Years in Trap C4

Chapter 5:

Conclusions and Future Work

I. Conclusions

i. Year-long Sediment Traps

Overall the yearlong sediment traps were strongly correlated to one another, indicating that this year, 2006-2007, was dominated by homopycnal flow. If the anomalies found in trap C1 did not result from sampling errors, then there may have been an interflow in Linnévatnet to the extent that more sediment reached the lower three traps as a result of water temperature and density.

This year was typified by an increasing sediment flux in each successively deeper trap. For each deeper trap, the grain size peaks were coarser than the previous trap. All the traps also increased at least slightly in grain size at the top of the traps.

Finally, changing sampling techniques for trap halves C1 and C1.2 did not yield any significantly differently results. The pattern in grain size increases and decreases remained the same.

ii. Spring Sediment Traps

Traditional spring trap Cbt mimics yearlong trap C4 very closely. Cbt does lack the finer sediment at the bottom of the trap, which helps to constrain the timing of deposition for C4. The first two coarsening peaks in Cbt and C4 are inverted, in the sense that the first peak in Cbt is finer than the first in C4, the reverse holds true for the second peak. This may be a result of the traps being only within 10m of each other, leaving them vulnerable to record slightly differing parts of an incoming turbidity event.

The modified coke bottled traps did not yield any significant insights into the efficiency of the currently used 'traditionally' designed traps. Though as far as the coke bottle design goes, the receiving tube had too large a diameter preventing me from obtaining detailed grain sized results. But comparing the modified traps to each other did reveal that having the baffle muted the signal of grain size changes, meaning the trap without the baffle had grain sizes that differed more.

iii. Environmental Conditions

All the significant turbidity spikes could be correlated to other events in the valley, including the thawing of the river, melting of the snow, and a combination of those two plus a precipitation event.

The turbidity graph could then be correlated to the grain size graphs: the three big turbidity spikes to the three coarsening events found in each trap. This correlation leaves the top portion of each trap, where the grain sizes begin to increase again, unaccounted for; such an increase may result from glacier ablation.

II. Future Work

As far as sampling the traps, the finer the subsample the better. This eliminates the question of honoring the stratigraphy, and gives very detailed graphs that, when similar, are almost mirror images of one another.

For the future, it may be beneficial to deploy a traditional trap without the baffle, to see if the observed effect in the coke bottle traps holds true for inclined funnel walls. I would not recommend switching to the coke bottle traps, both

because of the receiving tube size, and because no significantly different signal was identified. The message between the differently designed traps remained the same.

It may also be helpful to deploy temperature loggers all the way up the inflow stream to better monitor when the river becomes completely unfrozen. Such results may coincide nicely with the noticeable grain size increase at the top of the traps. If so, it argues for particle size increases to be a result of sediment being carried down from the glacier to Linnévatnet.

References

Benn, Douglas I. And Evans, David J.A. 1998. Glaciers & Glaciation. London: Arnold.

Ingólffsson, Ólafur. 2007. Outline of the geography and geology of Svalbard. http://www.hi.is/~oi/svalbard_geology.htm. (accessed February 29, 2008).

Intergovernmental Panel on Climate Change (IPCC) 2007. Climate Change 2007: Synthesis Report. Valencia, Spain, 12-17 November 2007. http://www.ipcc.ch/pdf/assessment-report/ar4/syr/ar4_syr.pdf (accessed May 2, 2008).

Ladvik, J.Y., Mangerud, J. and Salvigsen, O. 1987. The Late Weichselian and Holocene shoreline displacement on the west-central coast of Svalbard. *Polar Research* 5, 29-44.

McKay, N. *Characterization of Climatic influences on modern sedimentation in an Arctic lake, Svalbard, Norway.* Geological Society of America. Abstracts with Programs. 37 (1):29. 2005.

Motely, Brooks. 2006. Sedimentation in Linnévatnet, Svalbard during 2004-2005: a modern process study using sediment traps. *36th International Arctic Workshop Abstract*. **http://instaar.colorado.edu/meetings/AW2006/abstract_detail.php?abstract_id=15** (accessed March 22, 2008).

Nesje, Atle and Dahl, Svein Olaf. 2000. Glaciers and Environmental Change. London: Arnold.

Norsk Polarstitutt. 1936. Oblique Aerial Photograph from 1936 of Linnevatnet, Spitzbergen, Svalbard. http://instaar.colorado.edu/meetings/AW2006/abstract_detail.php?abstract_id=59

Perrault, L. 2006. Mineralogical Analysis of Primary and Secondary Source Sediments, Linnévatnet, Spitsbergen, Svalbard. Unpublished Bates College B.S. Thesis.

Pratt, E. 2006. Characterization and Calibration of Lamination Stratigraphy of Cores recovered from Lake Linné, Svalbard, Norway. Unpublished Mount Holyoke College B.A. Project.

Roop, Heidi. 2007. Sedimentation in a proglacial lake: Interpreting inter and intra-annual sedimentation in Linnévatnet, Spitsbergen, Norway. Unpublished Mount Holyoke College B.A. Thesis.

Sandahl, T. 1986. Kvartaergeologiske undersokelser I Omradet Lewinodden – Kapp Starostin – Linnevatnet ytre Isfjordern, Svalbard. Unpublished thesis, University of Bergen.

Sndyer, J.A. 2000. Holocene cirque glacier activity in western Spitzbergen, Svalbard: sediment records from proglacial Linnévatnet. The Holocene 10, no. 5: 555-563.

Svendsen, J.I., Mangerud, J., and Miller, G.H. 1989. Denudation rates in the

Arctic estimated from sediments on Spitsbergen, Svalbard.

Paleogeography, Paleoclimatology, Paleoecology 76, 153-68.

Appendix:

Mean vs Median vs Mode for Traps C1, C2, C3, Cbt and Cb/Cnb Grain Sizes

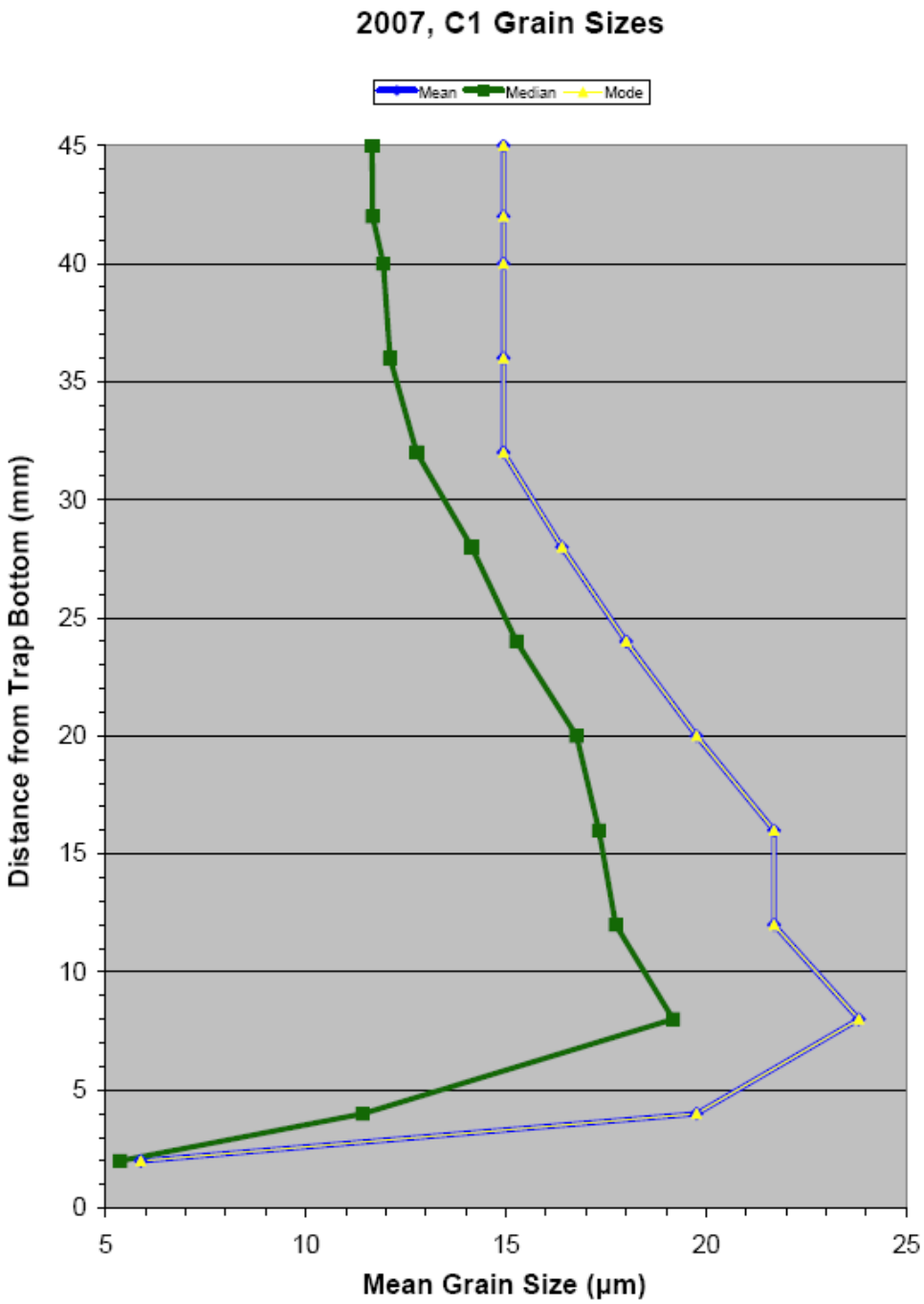

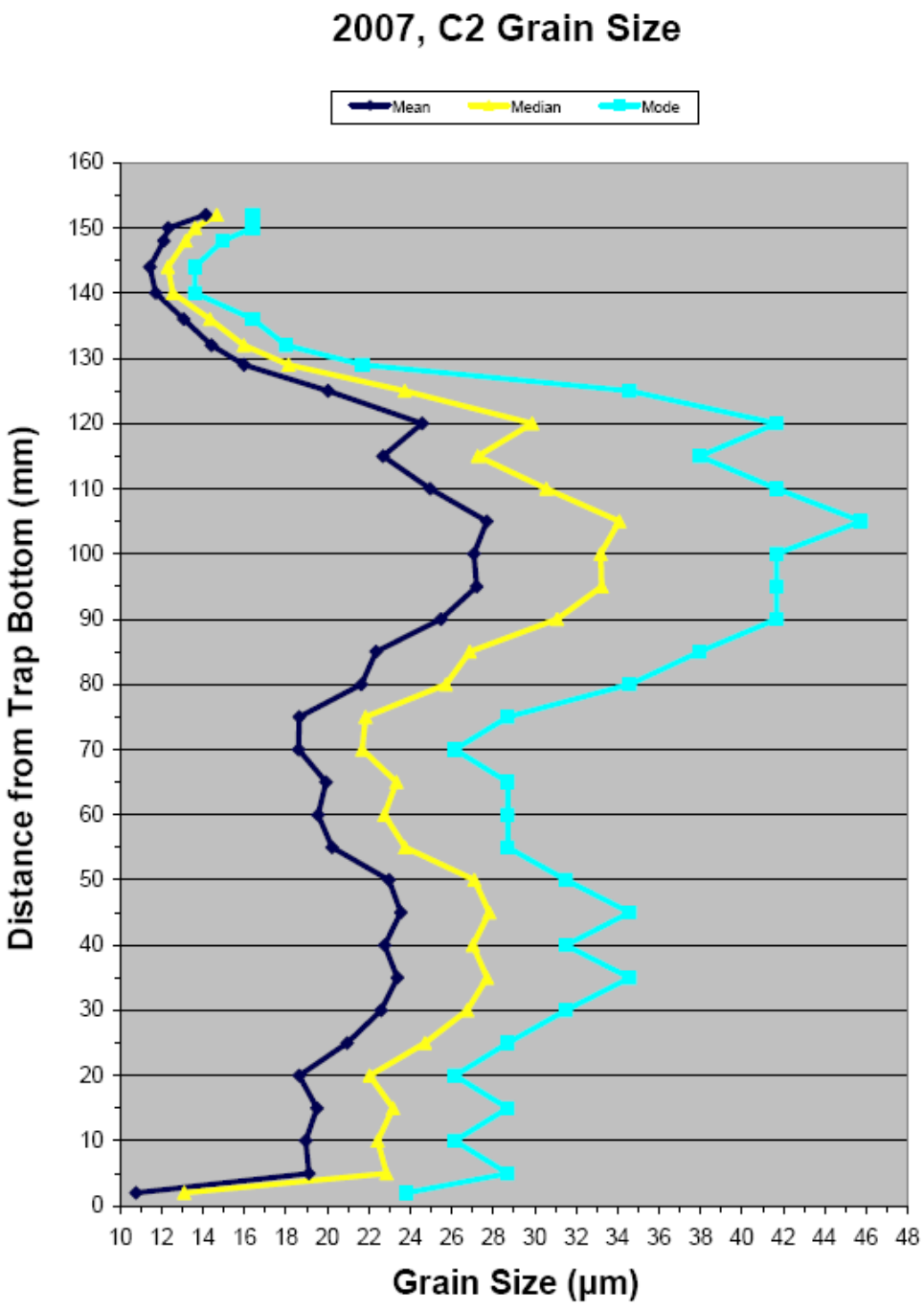
2007, C2 Grain Size
Mean
Median
Mode
Distance from Trap Bottom (mm)
0
10
20
30
40
50
60
70
80
90
100
110
120
130
140
150
160
10 12 14 16 18 20 22 24 26 28 30 32 34 36 38 40 42 44 46 48
Grain Size (µm)

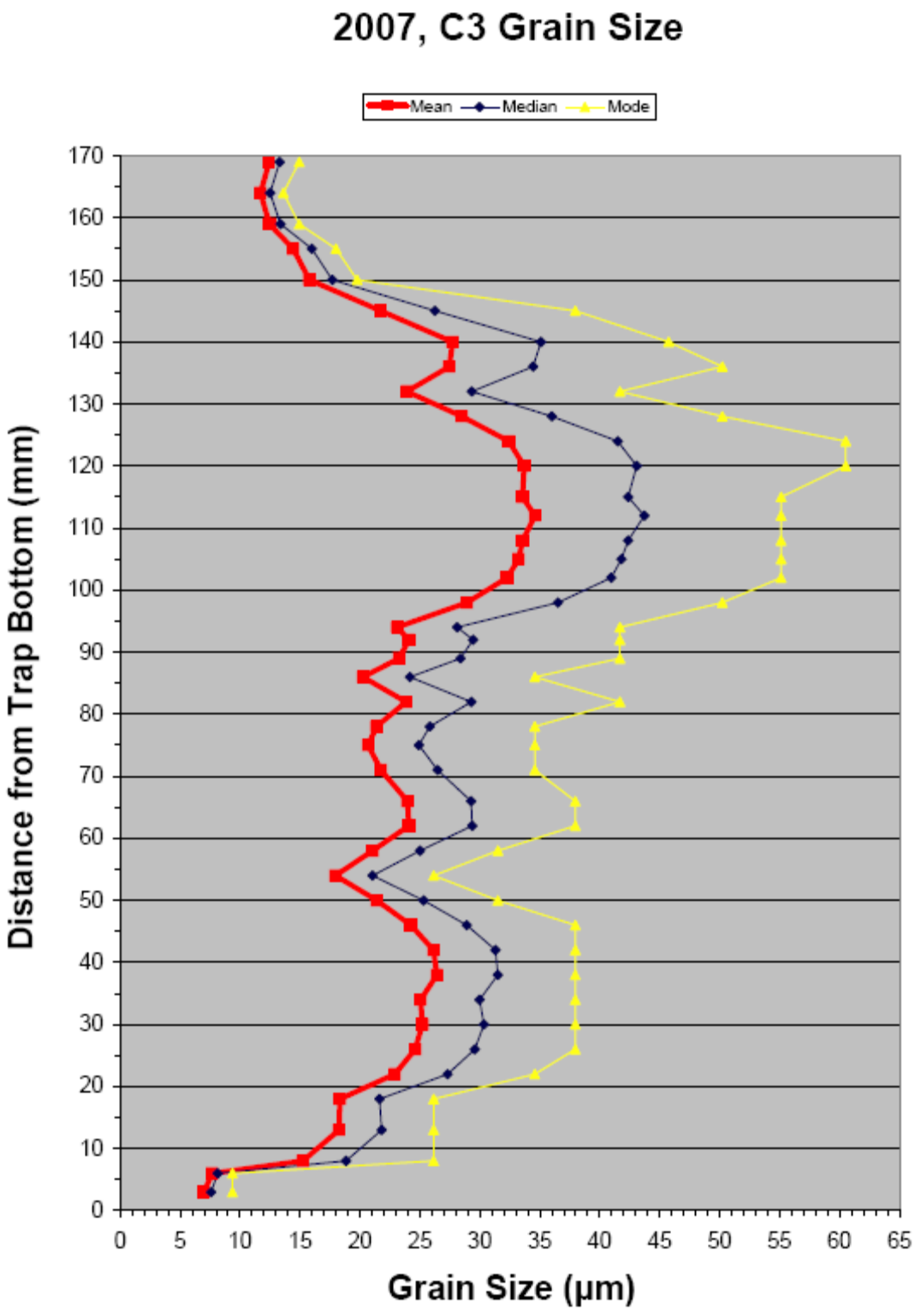
2007, C3 Grain Size
Mean
Median
Mode
Distance from Trap Bottom (mm)
0
10
20
30
40
50
60
70
80
90
100
110
120
130
140
150
160
170
0
5
10
15
20
25
30
35
40
45
50
55
60
65
Grain Size (µm)

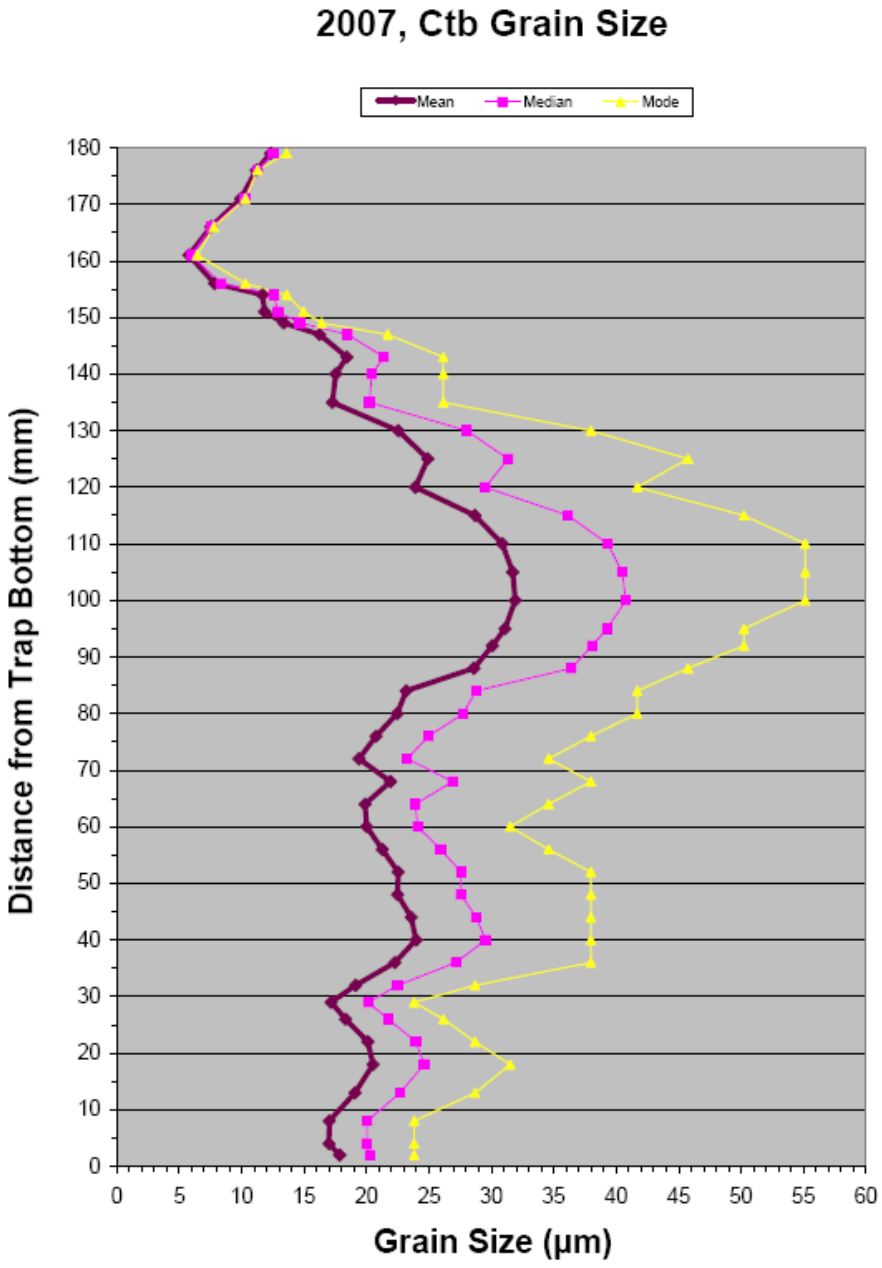
2007, Ctb Grain Size
Mean
Median
Mode
Distance from Trap Bottom (mm)
0
10
20
30
40
50
60
70
80
90
100
110
120
130
140
150
160
170
180
0
5
10
15
20
25
30
35
40
45
50
55
60
Grain Size (µm)

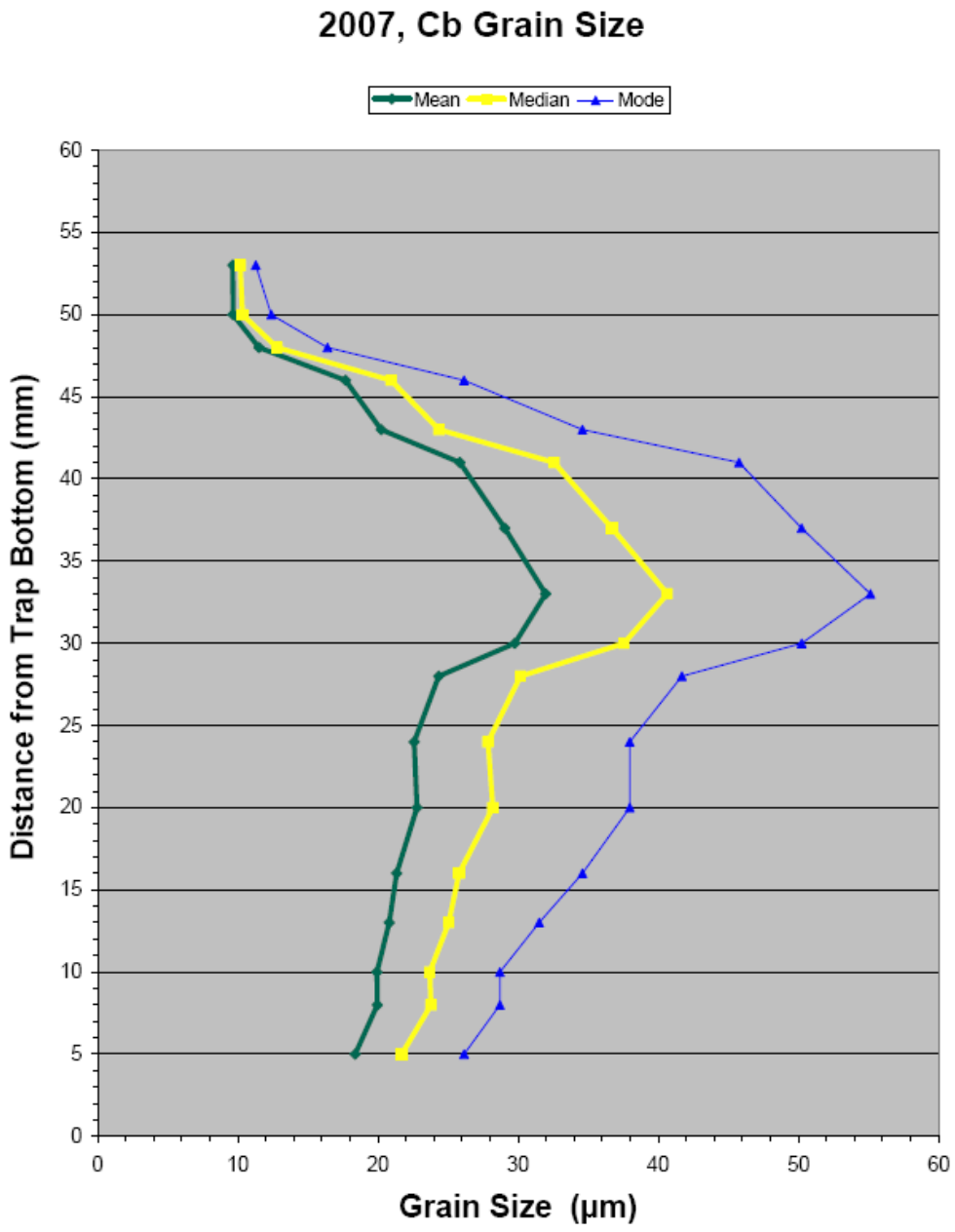
2007, Cb Grain Size
Mean
Median
Mode
Distance from Trap Bottom (mm)
0
5
10
15
20
25
30
35
40
45
50
55
60
0
10
20
30
40
50
60
Grain Size (µm)

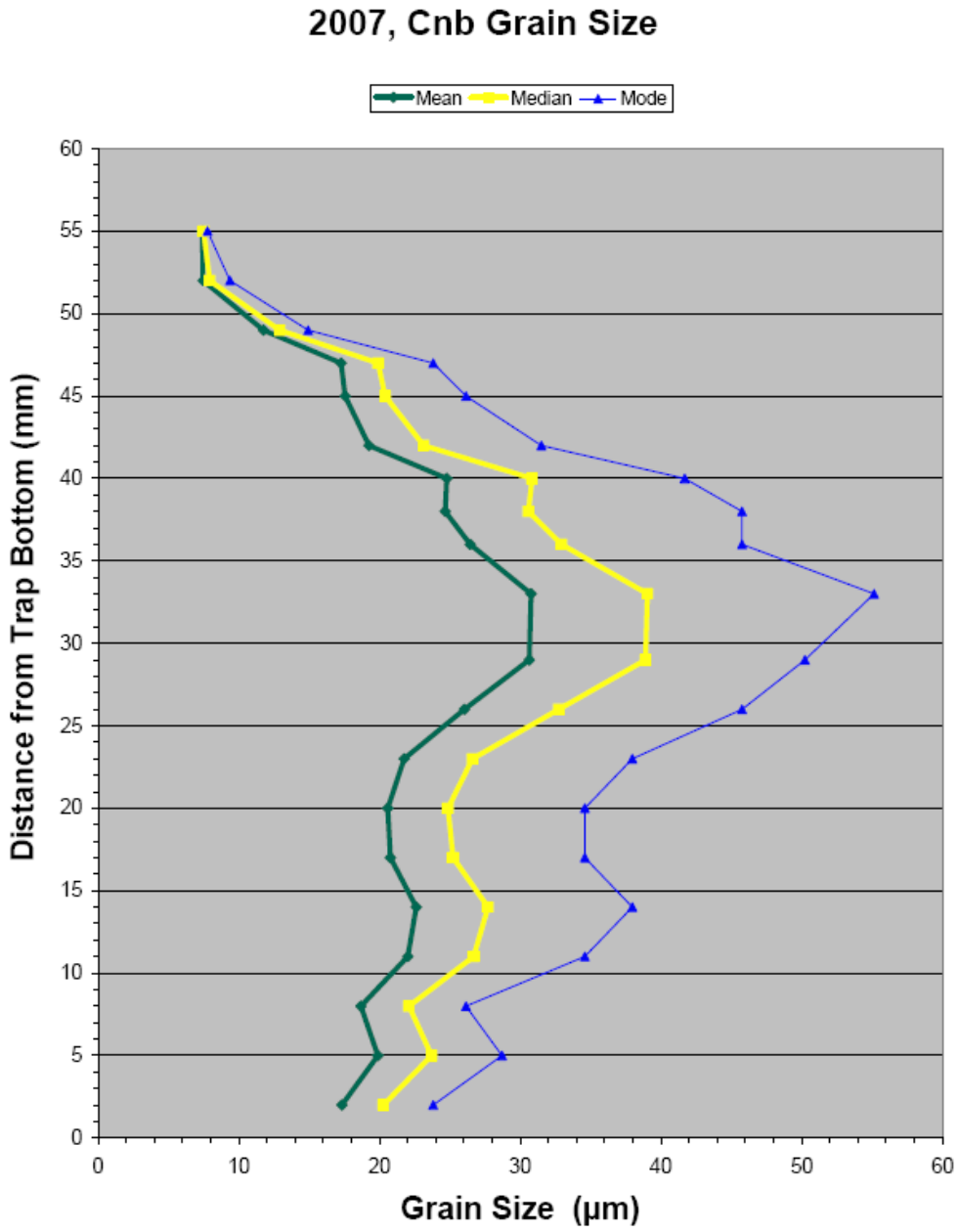
2007, Cnb Grain Size
Mean
Median
Mode
Distance from Trap Bottom (mm)
0
5
10
15
20
25
30
35
40
45
50
55
60
0
10
20
30
40
50
60
Grain Size (µm)

I give permission for public access to my thesis and for any copying to be done at the discretion of the archives librarian and/or the college librarian.

Patrice F. Cobin